Zoologica Scripta

Diversity of the snail-eating snakes *Pareas* (Serpentes, Pareatidae) from Taiwan

Chung-Wei You, Nikolay A. Poyarkov Jr & Si-Min Lin

Submitted: 22 October 2014
Accepted: 6 February 2015
doi:10.1111/zsc.12111

You C.-W., Poyarkov Jr N.A., Lin S.-M. (2015). Diversity of the snail-eating snakes *Pareas* (Serpentes, Pareatidae) from Taiwan. — *Zoologica Scripta*, *00*, 000–000.

Pareatidae are a group of mollusc-eating snakes widely distributed in South-eastern Asia. Due to their dietary specialization, the asymmetric dentition of pareatids has recently become an interesting issue in evolutionary biology. However, phylogenetic relationships and species diversity of pareatids are still poorly studied. A total of three *Pareas* species, *P. formosanus* (Van Denburgh 1909), *P. compressus* (Oshima 1910) and *P. komaii* (Maki 1931), have been reported for Taiwan. However, only *P. formosanus* is currently regarded as a valid species. Using mitochondrial sequence phylogeny, nuclear *c-mos* haplotype network, as well as multivariate morphometrics, we re-evaluated the taxonomic status of *Pareas* from Taiwan, the Ryukyus and adjacent regions. These lines of evidence showed congruent results for the coexistence of three *Pareas* species in Taiwan, with prominent genetic and morphological differentiation and differing level of dentition asymmetry. The currently used name *P. formosanus* should be applied only to the snakes with red iris, comparatively short lower jaw and totally smooth dorsal scales. An examination of the type material indicated that the name *P. compressus* should be regarded as a junior synonym of *P. formosensis sensu stricto*. *Pareas komaii* (Oshima 1910) is confirmed as a valid taxon with yellow iris, elongated lower jaw and strongly keeled dorsals. The third clade is characterized by a yellow iris, elongated lower jaw and weakly keeled dorsals. Despite their sympatric occurrence, every examined individual showed consistent grouping from mitochondrial, nuclear and morphological markers, indicating there is no gene flow among these three clades. Here, we describe the third clade as a new specie, *Pareas atayal* sp. nov.

Corresponding author: *Si-Min Lin, Department of Life Science, National Taiwan Normal University, No. 8, Sec. 4, Tingzhou Road, Taipei 111, Taiwan. E-mails: fish@ntnu.edu.tw; fishdna@ms31.hinet.net*

Chung-Wei You, Department of Life Science, National Taiwan Normal University, Taipei, Taiwan. E-mail: chungweiyou@gmail.com

Nikolay A. Poyarkov Jr, Department of Vertebrate Zoology, Biological Faculty, Lomonosov Moscow State University, Leninskiye Gory, GSP–1, Moscow 119991, Russia and Joint Russian-Vietnamese Tropical Research and Technological Center, South Branch, 3, Street 3/2, 10 District, Ho Chi Minh City, Vietnam. E-mail: n.poyarkov@gmail.com

Si-Min Lin, Department of Life Science, National Taiwan Normal University, Taipei, Taiwan. E-mail: fish@ntnu.edu.tw

Chung-Wei You and Nikolay A. Poyarkov contributed equally to this study.

Introduction

Pareatidae are a group of mollusc-eating snakes recently separated from Colubridae (Lawson *et al.* 2005; Vidal *et al.* 2007; Zaher *et al.* 2009; Pyron *et al.* 2011). The members of Pareatidae are small sized arboreal nocturnal snakes characterized by blunt snout, lack of mental groove and the absence of teeth on the anterior part of maxillary (Rao & Yang 1992; Guo & Deng 2009). These snakes are endemic to the Oriental Region with a wide distribution throughout tropical and subtropical Asia (Rao & Yang 1992). Seventeen species of Pareatidae in three genera are currently recognized: one species of *Aplopeltura* (*Ap. boa*), five species of *Asthenodipsas* (*As. laevis*, *As. lasgalenensis*, *As. malaccanus*, *As. tropidonotus* and *As. vertebralis*) and 11 species of *Pareas* (*P. boulengeri*, *P. carinatus*, *P. chinensis*, *P. formosensis*, *P. hamptoni*, *P. iwasakii*, *P. margaritophorus*, *P. monticola*, *P. nigriceps*, *P. nuchalis* and *P. stanleyi*) (Rao & Yang 1992; Ota *et al.* 1997a,b; Huang 2004; Jiang 2004a,b; Guo & Deng 2009).

In Taiwan, the first pareatid snake was described by Van Denburgh (1909) from a single specimen collected in 'Kanshirei' (=now Guanziling, Tainan, south-western Taiwan) as *Amblycephalus formosensis* (Van Denburgh 1909). One year later, Oshima (1910) published *Psammodynastes compressus* based on a single specimen collected from 'Kokwangai, Taihoku' (=now in Xindian, Taipei, northern Taiwan). Both species shared the common character of smooth dorsals. Owing to the morphological similarity, Oshima (1916) himself invalidated this species as a synonym of *A. formosensis*. The third and the final species, *Amblycephalus komaii*, was described by Maki (1931) based on two specimens from 'Arisan' (=now Alishan, Jiayi, south-western Taiwan). According to the original description, *A. komaii* could be distinguished from *A. formosensis* by its keeled dorsals and position of the supralabials in relation to the oculars (Van Denburgh 1909; Maki 1931; Ota *et al.* 1997b). Lue (1989) suggested validity of these two species and noted that the keeled (*A. komaii*) and unkeeled (*A. formosensis*) species were distributed to higher and lower elevations, respectively.

Except for the change of the genus from *Amblycephalus* to *Pareas* (Smith 1943; Taylor 1965; ICZN 1971; Williams & Wallach 1989), the taxonomic status of pareatid snakes in Taiwan has remained stable for several decades. Although both species were listed in the herpetofauna of Taiwan, diagnosis between the two remained problematic for most herpetologists. Having examined 27 specimens from Taiwan in addition to the holotypes of both species, Ota *et al.* (1997b) suggested that the relative position of supralabials and oculars is not a valid character for the subdivision of Taiwanese *Pareas*. Furthermore, the arrangement and degree of development of keels were found to be highly variable, so the authors concluded that *P. komaii* should be regarded as a junior synonym of *P. formosensis*.

Another controversy is the relationship between *P. formosensis* and its congeners in adjacent regions. Jiang (2004b) evaluated morphological characters between *P. formosensis* on Taiwan and *P. chinensis* (Barbour 1912) on mainland Asia based on the literature review. Due to the overlapping number of ventrals and subcaudals, Jiang (2004b) concluded that *P. chinensis* should be a synonym of *P. formosensis*. However, Guo *et al.* (2011) based on prominent divergence in mitochondrial and nuclear sequences and position in phylogeny regarded *P. chinensis* as a valid species.

Due to the specialized feeding habit and foraging behaviour, the evolutionary biology of *Pareas* has received much attention in recent years (Hoso & Hori 2006, 2008; Hoso 2007; Hoso *et al.* 2007, 2010). In the southern Ryukyus, these snakes were found to specialize and coevolve with their molluscan prey (Hoso *et al.* 2010). Considering the fact that most land snails are predominantly dextral (Vermeij 1975), specializations for foraging on dextral snails would be selectively advantageous for snail-eating specialists. Such natural selection forced an ancestor of pareatid snakes in southern Ryukyus to evolve an asymmetric jaw, which could be quantified by a higher mandibular tooth count from their right mandible over the left one. Furthermore, Hoso *et al.* (2007) also predicted that snail-eating *Pareas* spp. would have a more asymmetric mandibular tooth count than slug eaters, who do not need to handle the asymmetric food item.

Variation in prey preference of *Pareas* snakes from Taiwan was first noticed by Lin (2010, personal communication on his master thesis), who noted that the *Pareas* from high- and low-elevation regions in Taiwan show specific preference on slugs and snails, respectively. After a preliminary evaluation on the samples used in his experiments on preying behaviour, we further found that the *Pareas* populations in Taiwan could be preliminarily distinguished by their dorsal keels, colour of iris and the shape of the heads and jaws (Fig. S1). Snakes with a red iris have shorter lower jaws and feed mostly on slugs, whereas snakes with a yellow iris have elongated jaws and might be able to consume a higher variety of prey items. Such variation hinted that these populations of snakes might show a considerable degree of genetic, morphological and behavioural differentiation.

In this study, we aim to solve the long-lasting question on species and genetic diversity of *Pareas* snakes in the island of Taiwan and adjacent regions. For this purpose, we sampled these snakes throughout Taiwan. Specimens from neighbouring regions were also included in the analysis. Based on molecular data, including mitochondrial and nuclear sequences, as well as morphological data, we argue that there are three distinct *Pareas* species coexisting in Taiwan: two of them require taxonomic revision and the third form represents a species new to science.

Materials and methods

Sample collection

During 2009–2011, we obtained 79 individuals of *Pareas* snakes from 15 localities, covering most of the distribution in Taiwan and southern Ryukyus (Fig. 1; Table S1). Specimens were fixed in 10% formalin and preserved in 70% ethanol, and a sample of their muscle tissues were preserved in 95% ethanol. Types and referred materials are stored in the herpetological collections of the National Museum of Natural Science (NMNS), Taichung, Taiwan and the Zoological Museum of Moscow State University (ZMMU), Moscow, Russia.

We collected four *Pareas* species from adjacent regions and included genetic information on seven species available

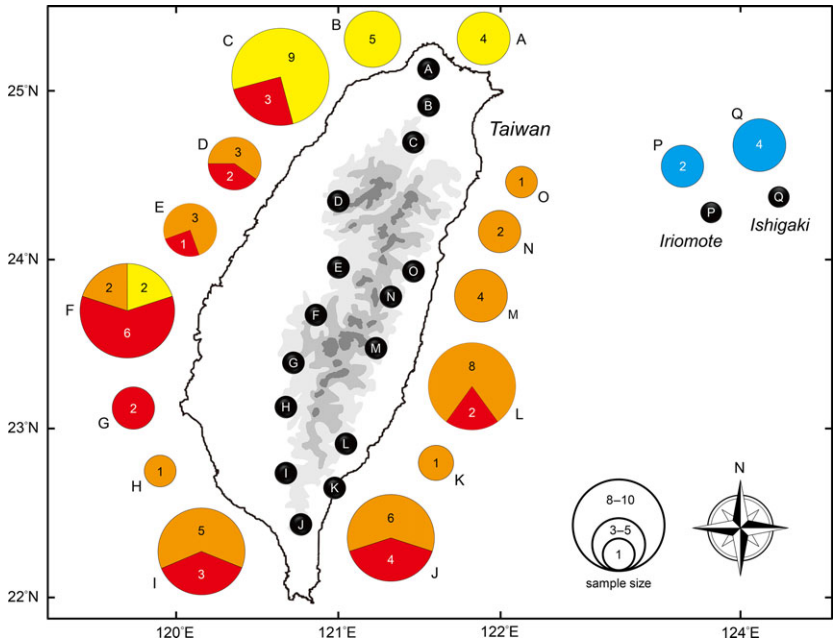

Fig. 1 Sample localities (A–Q) of *Pareas* samples used in this study. The pie charts represented the ratio and sample size of the red-eyed form (*P. formosensis*, in red), yellow-eyed form 1 (*P. komaii*, in orange), yellow-eyed form 2 (*P. atayal* sp. nov., in yellow) and *P. iwasakii* (blue).

from GenBank to reconstruct the phylogeny of *Pareas* (Table S1). Our collection included five *P. iwasakii* tissues: three from Ishigaki island and two from Iriomote island (locality P and Q in Fig. 1), provided by Dr. Masaki Hoso (Kyoto University, Japan); three *P. hamptoni*: two from Vietnam and one from Guangdong Province, China; three *P. margaritophorus*: two from Vietnam and one from Hong Kong; and two *P. carinatus* from southern Vietnam. Sequences downloaded from GenBank included *P. boulengeri*, *P. chinensis*, *P. macularius*, *P. monticola*, *P. stanleyi* and *P. hamptoni* (identified as *P. tonkinensis*; Guo *et al.* 2011; Ding *et al.* 2011; Fernandes & Malhotra 2003, direct submission sequence; see Table S1). The remaining members of Pareatidae, *Asthenodipsas tropidonotus*, *Asthenodipsas vertebralis* and *Aplopeltura boa*, served as outgroups.

Molecular techniques

Genomic DNA was extracted from ethanol preserved tissues using the EasyPure genomic DNA spin kit (Bioman, Taiwan) according to the manufacturer's instructions and stored at −20 °C until further usage. Complete mitochondrial cytochrome *b* gene and nuclear c-mos gene sequences were amplified by polymerase chain reactions (PCR). The primers used for cytochrome *b* amplification were as follows: L14910: 5′-GAC CTG TGA TMT GAA AAA CCA YCG TTG T-3′ and H16064: 5′-CTT TGG TTT ACA AGA ACA ATG CTT TA-3′, designed by De Queiroz *et al.* (2002). Primers used for amplification of nuclear c-mos gene were as follows: S77: 5′-CAT GGA CTG GGA TCA GTT ATG-3′and S78: 5′-CCT TGG GTG TGA TTT TCT CAC CT-3′, designed by Slowinski & Lawson (2002). Reactions were conducted in a 20-μL reaction volume containing 1× PCR buffer [10 mM Tris-HCl, pH 9.0; 50 mM KCl, 0.01% (w/v) gelatine and 0.1% Triton X-100], 0.8 U Taq DNA polymerase (Amersham Biosciences), 0.2 μM each primer, 0.5 mM dNTP and 50 ng template DNA. The PCR conditions were denaturation at 94 °C for 3 min, followed by 35 cycles at 94 °C for 30 s, 52 °C for 40 s and 72 °C for 90 s, with a final extension at 72 °C for 10 min using an iCycler Thermal Cycler (Bio-Rad). PCR products were purified with a PCR Product Pre-Sequencing Kit (USB Corporation) and subsequently used as the template for direct DNA sequencing reactions with a DYEnamic ET Dye Terminator Cycle Sequencing Kit (Amersham Pharmacia Biotech). The same primers used for PCR were used for the sequencing reactions. Sequencing products were run on an ABI 3730 automated DNA sequencer (Amersham Biosciences). The sequences were determined in both directions, and the original signals were proofread using Sequencher 4.7 (Gene Codes Corporation).

For nuclear c-mos gene, with possibly two alleles from this diploid locus, we used the PHASE algorithm (Stephens *et al.* 2001; Stephens & Scheet 2005) performed in software DNASP 5.10.1 (Librado & Rozas 2009) to reconstruct the two haplotypes of each individual from population genotype data. We implemented one million of Monte Carlo Markov Chain (MCMC) iterations while thinning at every 100 steps and discarding the first 1000 samples as burn-in. We excluded haplotypes for which phases were determined with probability <60% (Sotka *et al.* 2004).

Phylogenetic analyses of mitochondrial sequences

The obtained sequences were aligned by CLUSTAL W using MEGA 6.0.5 (Tamura *et al.* 2013). The data set after alignment contained 112 OTUs with 1119 bp, including 619 and 510 variable and parsimony-informative sites, respectively. PARTITIONFINDER 1.0.1 (Lanfear *et al.* 2012) was used to determine the best substitution model and partitioning scheme based on Bayesian information criterion (BIC) scores. The results indicated a scheme with three partitions: 1st, 2nd and 3rd positions. The preferred evolutionary model for all three partitions was TrN + I + G (Tamura–Nei's model with a proportion of invariable sites and a gamma distribution shape parameter).

The best partitioning scheme was then used for maximum likelihood (ML) and Bayesian phylogeny inferences. The ML analysis was conducted with RAXML 7.3.2 software (Stamatakis 2006). The best ML tree was selected from 200 iterations, each starting with distinct randomized parsimony trees. Clade support was examined by nonparametric bootstrap analyses (1000 replicates) summarized with 50% majority rule consensus trees. Bayesian inference analyses were conducted with MRBAYES 3.2.2 (Ronquist *et al.* 2012). The combined data matrix was partitioned, and models were assigned as suggested by PARTITIONFINDER. Two independent runs of 5×10^7 generations with eight MCMC chains each were conducted simultaneously, starting from random trees and resampling each tree every 1000 generations. The standard deviation of split frequencies between runs (<0.01) and the effective sample size (ESS) as measured by TRACER 1.5 (Rambaut & Drummond 2009) were monitored to ensure stationarity, convergence and correct mixing of the chains and to determine the correct number of generations to discard as a burn-in for the analyses (first 20%). Converged MRBAYES runs were combined after the exclusion of burn-in, and a majority rule consensus tree was created with nodal confidence assessed by posterior probabilities. Finally, the values of statistical supports from ML bootstraps and BPPs were labelled on corresponding nodes.

Haplotype network of nuclear c-mos gene

Owing to the comparatively lower sequence divergence of the c-mos gene, we conducted haplotype network to represent the interrelationship among *Pareas* species from Taiwan and adjacent regions. From 80 individuals, we obtained 160 c-mos partial sequences each of 602 bp in length. The 160 sequences contained 16 variable and 13 parsimony-informative sites, respectively. Individual sequences were transformed to haplotype data set by DNASP 5.10.1 (Librado & Rozas 2009), yielding to 13 haplotypes. Haplotype network was constructed using NETWORK 4.6.1.2 (Fluxus Technology Ltd.), where the size of the circles denoted the relative sample size.

Morphological examination and multivariate morphometrics

Morphological data for comparisons are based on examination of original collections by the authors and on information available in the literature and includes data from Pope (1935), Smith (1943), Nakamura & Uéno (1963), Taylor (1965), Rao & Yang (1992), Manthey & Grossmann (1997), Ota *et al.* (1997a,b), Cox *et al.* (1998), Zhao *et al.* (1998), Stuebing *et al.* (1999), Grossmann & Tillack (2003), Jiang (2004a,b), Guo & Deng (2009) and Das (2010).

Morphological description, measurements and scale counts follow Dowling (1951), Guo & Deng (2009) and Vassilieva *et al.* (2013). The terminal scute is excluded from the number of subcaudals. The numbers of dorsal scale rows are counted at one head length behind the head, at midbody and at one head length before the vent. Values for symmetric head characters are given in left/right order. Scale counts and measurements were taken under an Olympus SZ30 or Leica EZ4 microscopes using a digital caliper.

The hemipenal morphology was studied on specimens with hemipenal structures everted before preservation; terminology and description follow Keogh (1999). Cranial osteology of the new species (holotype NMNS 05594 and paratype ZMMU R-14434) was investigated with kind help of Dr. Masaki Hoso (Kyoto University, Japan) using high-resolution X-ray computed tomography (voxel size 10 mm); images were processed using MESHLAB 32 bit v 1.3.3.

The following measurements and counts were taken: snout-vent length (SVL); tail length (TaL); total length (TL); head length (HL, from snout tip to jaw angles); head width (HW); head height (HH); interorbital distance (IO); eye–nostril distance (EN, from anterior edge of orbit to posterior edge of nostril); internarial distance (IN); eye diameter (ED, horizontal); snout length (SnL, from the tip of rostral to the anterior margin of eye); nasal scale (NAS, entire or divided); supralabial scales (SL); infralabial scales (IL); loreal scale(s) (LOR); pre-ocular scales (Pre-OC); postocular scales (Post-OC); temporal scales (Temp); dorsal scale rows (DSR), including number of dorsal scale rows at neck (ASR, about one HL behind head); number of dorsal scales at midbody (MSR, at number of VEN/2); number of dorsal scale rows before vent (PSR); number of keeled dorsal scale rows at neck (KAD); number of keeled dorsal scales at midbody (KMD); number of keeled dorsal scale rows before vent (KPD); ventral scales (VEN); subcaudal scales (SC); and anal scale (entire or divided). Numbers of pattern units (like crossbars or vertebral blotches) are provided as number on body + numbers on tail.

We performed principal component analysis (PCA) and discriminant analysis (DA) to discriminate among the

genetic clades from Taiwan and the Ryukyus. First, we obtained morphological data from 62 intact individuals with clade groupings confirmed by molecular phylogeny. After preliminary tests, we chose nine traits which could provide a best resolution among the clades, including six meristic characters (IL, VEN, SC, KAD, KMD and KPD) and three size-related traits (TaL/TL, HL/TL and SnL/HL). PCA and DA were performed using JMP 7.0 (SAS Institute Inc.)

After PCA and DA have been executed, a series of coefficients was determined which could best discriminate the clades according to linear composition of characters from each individual. We took the same characters from the holotype (NSMT H00529) and the paratype (NSMT H00530) of *Pareas komaii*, and the specimen NSMT H02567 which might represent the type of *Psammodynastes compressus* Oshima 1910 preserved in National Science Museum, Tokyo, Japan. Characters taken from these type specimens were calculated with coefficients by linear composition to obtain their relative position in the scatter plots in PCA and DA.

Results

Genetic differentiation among Taiwanese Pareas

Phylogeny of cytochrome *b* gene reconstructed by ML and Bayesian approaches yielded to the same tree topology with high statistical supports on each node (Fig. 2A). Therefore, we took the ML tree as the best topology explaining the interrelationship among Taiwanese samples. The species of *Pareas* from East Asian islands (Taiwan and southern Ryukyus) group together with *P. hamptoni* distributed in mainland Asia. We refer to this clade as '*P. hamptoni*

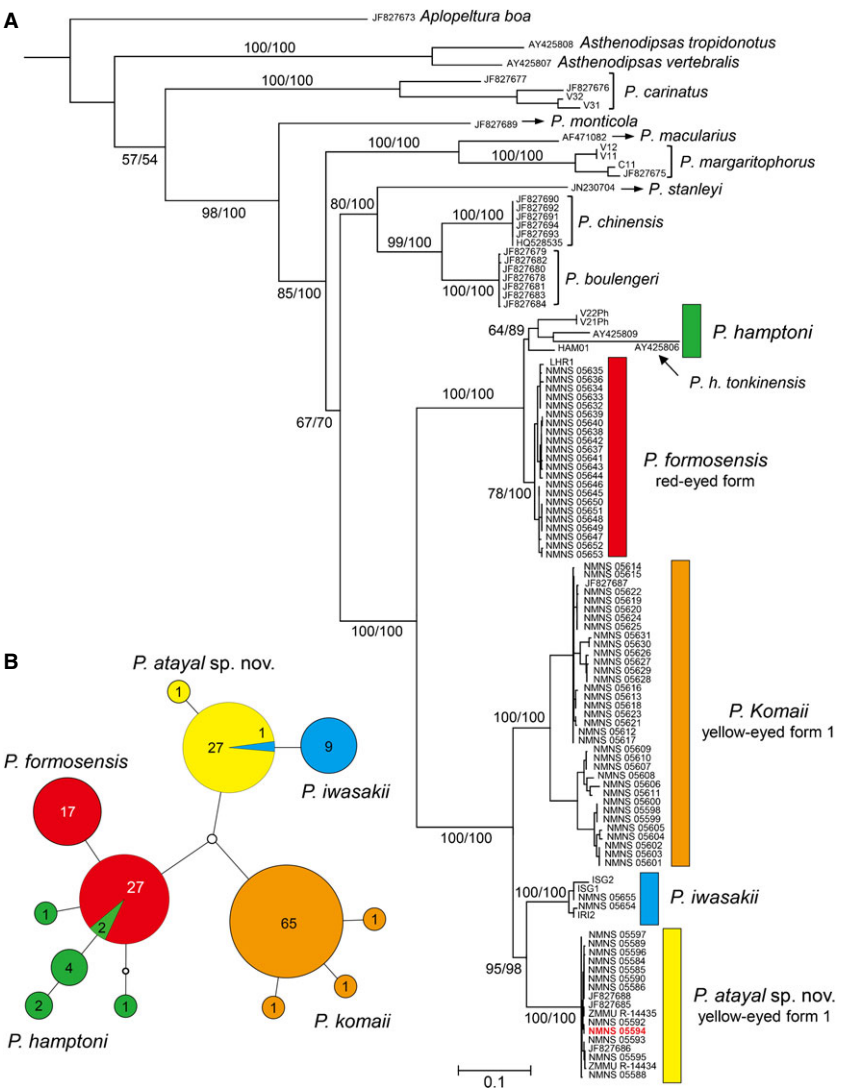

Fig. 2 (A) Maximum-likelihood (ML) tree of *Pareas* species constructed using mitochondrial cytochrome *b* sequences (1119 bp, full length). Numbers above each node denote the statistic support from 1000 ML replicates and Bayesian posterior probabilities. (B) Haplotype network of nuclear c-mos gene from the 160 haplotypes (80 individuals) of *Pareas* species in Taiwan and southern Ryukyu. The areas of the circles correspond to the samples, while the colours correspond to the clade assignment in the phylogenetic tree. Green: *P. hamptoni*; red: the red-eyed form (*P. formosensis*); orange: the yellow-eyed form 1 (*P. komaii*); blue: *P. iwasakii*; and yellow: the yellow-eyed form 2 (*P. atayal* sp. nov.).

group' in the following discussion. *Pareas* in Taiwan were divided into three distinct clades (noted as red, orange and yellow bars in Fig. 2A) and did not form a monophyly. Specimens with red iris, short lower jaws and smooth dorsals (denoted with the red bar) were closely related to *P. hamptoni* collected from Guagdong (HAM01), from Vietnam (V21Ph and V22Ph) and AY425809 from GenBank (sample location not available). *Pareas tonkinensis* from GenBank is included in the *P. hamptoni* clade. Specimens with yellow iris, elongated lower jaws and keeled dorsals were further assigned into two clades. Snakes with stronger keels and higher keeled dorsal rows formed a unique clade, while those with weaker keels and lower number of keeled dorsals were grouped with *P. iwasakii*. These two clades were defined as 'yellow-eyed form 1' and 'yellow-eyed form 2', respectively. This branching pattern persisted with high statistical support among different analyses.

Sequence divergence among the clades has reached the species level and even exceeded interspecific divergence among some of the other *Pareas* species (Table S2). The two yellow-eyed clades have a divergence of 0.1085, whereas the distance between the red-eyed clade and the two yellow-eyed clades is 0.1810 and 0.1759, respectively. These values exceed genetic distances among *P. boulengeri*, *P. chinensis* and *P. stanleyi* (divergence from 0.1013 to 0.1702; Table S2).

Haplotype network of the 160 nuclear c-mos sequences is given in Fig. 2B, with the area of each haplotype corresponding to its sample size. We report a precise consistency between mitochondrial and nuclear groupings of Taiwanese *Pareas*. Individuals of red-eyed form, yellow-eyed form 1 and yellow-eyed form 2 have unique haplotypes, with at least two mutation steps from each other which are not shared by the other clades. Shared nuclear haplotypes were revealed in two sister pairs: between *P. iwasakii* and the yellow-eyed form 2, where a heterozygous *P. iwasakii* showed one allele identical to the most common one from the latter; and between *P. hamptoni* and the red-eyed form, where two *P. hamptoni* had one allele identical to the latter (Fig. 2B). Thus, although with a large area of sympatric occurrence (Fig. 1), species do not share nuclear haplotypes with the other clades even when they come into contact.

Morphological analyses

All Taiwanese samples could be correctly assigned into morphological groups congruent with their molecular clades (Fig. 3). The PCA ordination plot successfully separated the three groups of snakes, where the first two principal component eigenvectors accounted for 64.72% of variation (Fig. 3A). Similarly, all groups were recovered in DA and each individual could be 100% correctly assigned to its phylogenetic clade (Fig. 3B). All snakes belonging to red-eyed clade shared the characters of red iris, short head, short lower jaw and smooth dorsals; while the yellow-eyed forms have yellow iris, longer head, elongated lower jaw and keeled dorsals (Fig. 4). The yellow-eyed form 2 could be further distinguished from form 1 by its higher numbers of infralabial scales (IL = 8.59 ± 0.59 vs. 7.81 ± 0.65, $P = 0.0013$), ventral scales (VEN = 180.77 ± 4.55 vs. 174.27 ± 4.67, $P = 0.0002$) and subcaudal scales (SC = 75.47 ± 2.23 vs. 69.56 ± 3.84, $P < 0.0001$; Table 1). Yellow-eyed form 1 has significantly higher numbers of keeled dorsal rows in every position of the body (KAD, KMD and KPD) than form 2 (Table 1).

Following the formula of PC1 and PC2 provided by PCA, and dim 1 and dim 2 provided by DA, the specimen NSMT H02567 (which represents the type of *Psammodynastes compressus* Oshima 1910; see Discussion) clearly clusters within the red-eyed form. On the other hand, both the holotype and the paratype of *P. komaii* were both assigned to the yellow-eyed form 1 group (Fig. 3). This indicates

Table 1 Measurements and meristic characters of *Pareas formosensis* (the red-eyed form), *P. iwasakii*, *P. komaii* (the yellow-eyed form 1) and *P. atayal* sp. nov. (the yellow-eyed form 2) represented by mean ± SD

Characters	*P. formosensis* (*n* = 13)	*P. iwasakii* (*n* = 4)	*P. komaii* (*n* = 34)	*P. atayal* (*n* = 17)
IL	6.65 ± 0.59 (6–8)	9.75 ± 0.87 (9–11)	7.81 ± 0.65 (6–9)	8.59 ± 0.59 (7–9)
VEN	174.85 ± 3.08 (170–180)	192.00 ± 1.41 (190–193)	174.27 ± 4.67 (162–182)	180.77 ± 4.55 (174–188)
SC	74.15 ± 3.58 (69–82)	79.00 ± 3.83 (76–84)	69.56 ± 3.84 (60–76)	75.47 ± 2.23 (71–79)
KAD	0 ± 0 (0–0)	1.5 ± 1.73 (0–3)	4.82 ± 2.15 (0–9)	0.47 ± 1.01 (0–3)
KMD	0 ± 0 (0–0)	6.00 ± 2.00 (3–7)	10.18 ± 1.91 (7–13)	5.94 ± 1.60 (3–9)
KPD	0 ± 0 (0–0)	8.00 ± 1.15 (7–9)	11.41 ± 1.54 (9–13)	6.18 ± 1.42 (3–9)
TaL/TL	0.23 ± 0.01 (0.21–0.25)	0.23 ± 0.01 (0.21–0.24)	0.22 ± 0.01 (0.20–0.25)	0.23 ± 0.02 (0.21–0.27)
HL/TL	0.029 ± 0.002 (0.026–0.033)	0.034 ± 0.003 (0.031–0.039)	0.036 ± 0.003 (0.031–0.047)	0.035 ± 0.003 (0.031–0.040)
SnL/HL	0.29 ± 0.02 (0.26–0.32)	0.20 ± 0.01 (0.19–0.21)	0.23 ± 0.02 (0.20–0.26)	0.24 ± 0.02 (0.22–0.28)

IL, infralabials; VEN, ventrals; SC, subcaudals; KAD, number of keeled dorsal scale rows at neck; KMD, number of keeled dorsal scale rows at midbody; KPD, number of keeled dorsal scale rows before vent; TaL, tail length; TL, total length; HL, head length (from snout tip to jaw angles); SnL, snout length (from the tip of rostral to the anterior margin of eye).

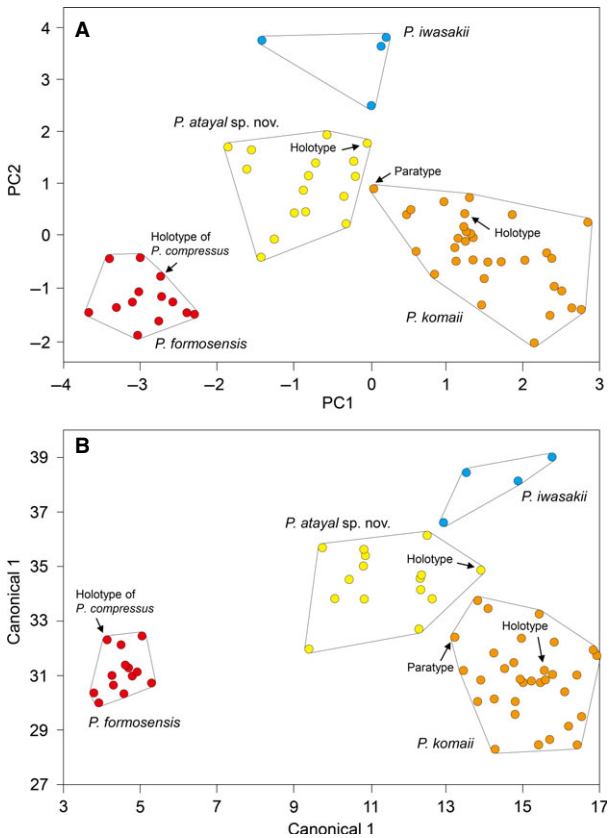

Fig. 3 Principle component analysis (A) and discriminate analysis (B) from morphology of *Pareas* species in Taiwan and southern Ryukyu. Green: *P. hamptoni*; red: the red-eyed form (*P. formosensis*); orange: the yellow-eyed form 1 (*P. komaii*); blue: *P. iwasakii*; and yellow: the yellow-eyed form 2 (*P. atayal* sp. nov.).

that (i) the specimen Oshima (1910) used in his description of *P. compressus* does not differ from specimens of the red-eyed clade (*P. formosensis*); (ii) the name *P. komaii* should be applied to the yellow-eyed form 1; and (iii) the yellow-eyed form 2 should be treated as a new species.

Morphological variation and dentition asymmetry

Mean and standard errors of the nine diagnostic characters are listed in Table 1, showing that *P. iwasakii* has largest numbers of infralabials (9.75 ± 0.87), ventrals (192.00 ± 1.41) and subcaudals (79.00 ± 3.83). In contrast, *P. formosensis* has lowest numbers of infralabials (6.65 ± 0.59) and ventrals (174.85 ± 3.08), and *P. komaii* has fewest subcaudals (69.56 ± 3.84). The strongly keeled dorsals of *Pareas komaii* are represented by the highest number of keeled dorsal rows (KAD, KMD and KPD), *P. formosensis* is entirely unkeeled. The ratio of tail length to total length (TaL/TL) did not show significant difference among the four species; yet *P. formosensis* has the lowest ratio of head length to tail length (HL/TL = 0.029 ± 0.002), compared to HL/TL > 0.034 in the other species. Differences in head shape were also shown by the differences in the SnL/HL ratio: *P. formosensis* exhibited the highest ratio (indicating the shortest lower jaw; Fig. S1), and *P. iwasakii* represented the lowest (the longest lower jaw; also see Fig. 4 for comparison).

Samples from the three *Pareas* clades in Taiwan also possess differing mandibular teeth counts and asymmetry indices (Table S3). The *P. formosensis* specimen we evaluated has 18 teeth in right mandible and 13 in left, yielding to an index of 16.13, precisely identical to the value proposed by Hoso *et al.* (2007). The two *P. komaii* has 21 teeth in right and 16–18 in left, yielding to 7.69–13.51 asymmetry index, appearing to be one of the most mandibularly symmetric *Pareas* species compared to congeners. *Pareas* sp. nov. has 20 in right, and 11 (holotype, NMNS 05594)—13 (one of the paratypes, ZMMU R-14434) in left (Fig. S2). Asymmetry index of this clade was 21.21 in one of the paratypes and could reach to 29.03 in holotype, ranking as the most asymmetric among all pareatid snakes studied to date.

Discussion

The highly congruent results from morphology and molecular data indicate the presence of three highly divergent clades which are clearly diagnosable in morphological characters. Such deep differentiation within the Taiwanese *Pareas* contradicts the results of the last review by Ota *et al.* (1997b), who concluded that all Taiwanese populations should be treated as a single species, *P. formosensis* (Van Denburgh 1909). It is worthy to note that two or more *Pareas* clades occur sympatrically at seven of the 15 sites sampled. However, samples collected from these sites never showed evidence of introgression, indicating that these species do not hybridize even when they are in contact in nature. Furthermore, we noticed that all the sampling sites with more than five individuals represent occurrence of at least two different clades, suggesting that coexistence of two or more pareatid species might be common throughout the island.

The name P. formosensis should be applied only to the red-eyed form

Both the original description of Van Denburgh (1909) and the re-evaluation by Ota *et al.* (1997b) of the holotype of *P. formosensis* indicated that this snake is characterized by its smooth dorsal scales. Although we did not have a chance to check the holotype of *P. formosensis* preserved in California Academy of Sciences (CAS 18006), the photograph provided by Ota *et al.* (1997b) clearly shows that this specimen is a smooth-scaled snake with short head and jaw. According to our study, these characters are found only in the red-eyed clade of Taiwanese *Pareas*. Based on these lines of evidence,

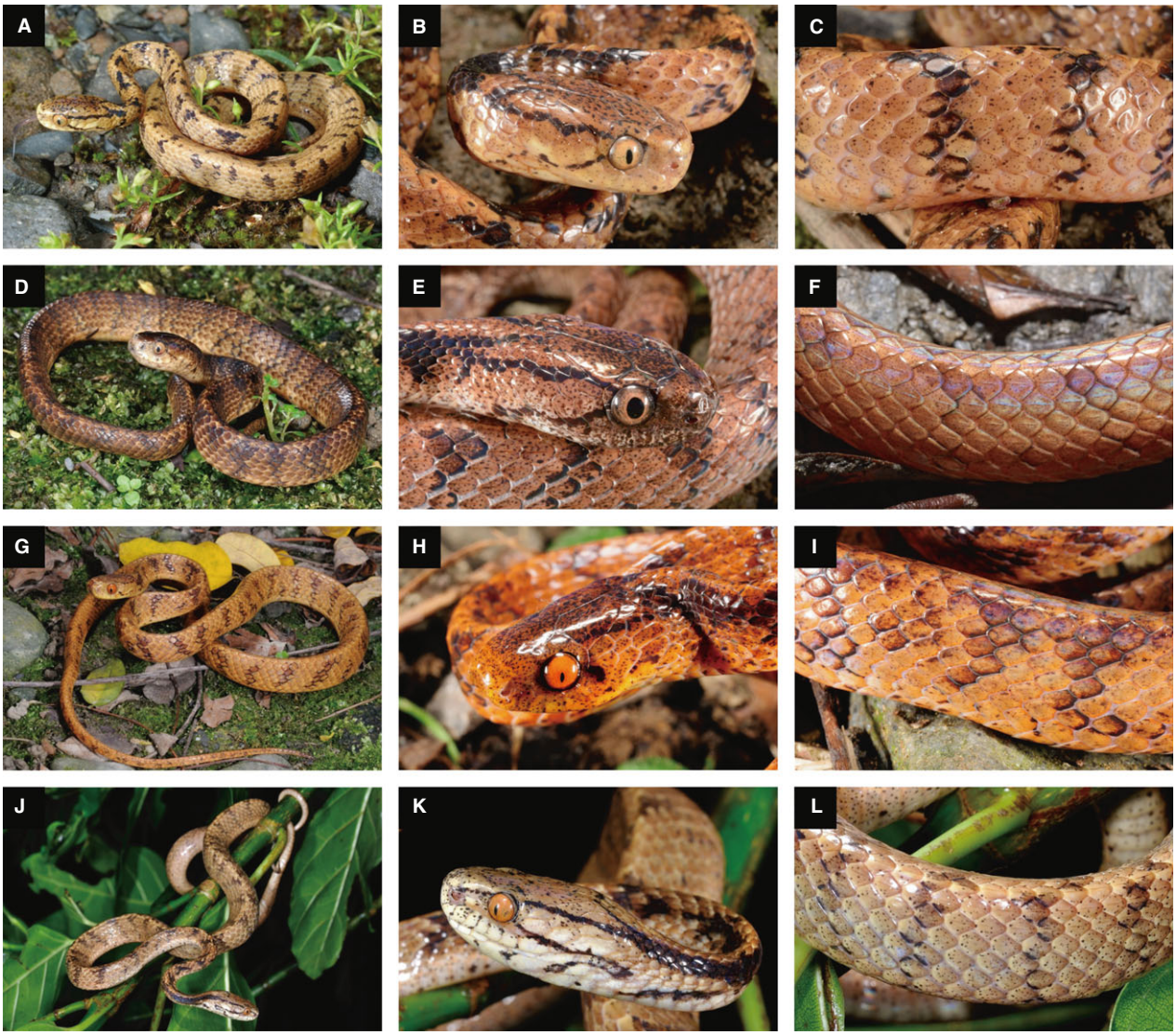

Fig. 4 A comparison of body coloration, iris coloration and scales among *Pareas atayal* sp. nov., *P. komaii*, *P. formosensis* and *P. iwasakii*. *Pareas atayal* sp. nov. is characterized by its yellow iris and slightly keeled dorsals (A, B, and C); *P. komaii* is characterized by its yellow iris, strongly keeled dorsals and usually darker coloration (D, E and F). *Pareas formosensis* is especially distinguishable from the formers by its red iris and totally smooth dorsals (G, H and I), and *P. iwasakii* is distinguishable by its extra-elongated head and jaw (J, K and L). Photographed by C.-W. You.

we conclude that the name *P. formosensis* (Van Denburgh 1909) should be applied only to the red-eyed taxon.

However, the taxonomic status of *P. hamptoni* in different regions remains a controversial issue. *Pareas hamptoni* has wide distribution in South-east Asia from Myanmar to Thailand, Indochina and southern China (Yunnan, Hainan, Guangdong and Guangxi provinces) in the east (Nguyen *et al.* 2009). The mean divergence of cytochrome *b* sequences within this species is 0.0513, comparable to the level of differentiation between *P. formosensis* and *P. hamptoni* (0.0571). Such high divergence indicates that *P. hamptoni* might represent a complicated species complex with pronounced geographic structure. Furthermore, although the name *P. tonkinensis* has been treated as a synonym of *P. hamptoni* in some recent literature (Nguyen *et al.* 2009) or as a subspecies *P. h. tonkinensis* (Orlov *et al.* 2000), the long branch of *P. h. tonkinensis* in the phylogenetic tree makes their taxonomy more problematic. Despite this potential problem, none of the recent studies (including this one) included the specimens or tissues from the *P. hamptoni* type locality, Mogok (Myanmar) or provided a detailed description of the holotype of this species. The

original description of *P. hamptoni* mentioned that dorsals are 'feebly keeled' (Boulenger 1905), yet this character did not show up in Chinese nor Vietnamese samples in our disposal (all specimens have completely smooth dorsals). The samples collected across Vietnam, China and Taiwan should not represent typical morphology of *P. hamptoni*.

Considering the fact that *P. formosensis* represents a reciprocally monophyletic group in respect to *P. hamptoni* samples in our study (Fig. 2A), we can offer two probable taxonomic treatments: (i) If *P. hamptoni* is defined as a widely distributed species with huge geographic differentiation in morphology, the Taiwanese population could be treated as a local subspecies, that is *P. hamptoni formosensis*. (ii) If topotypic *P. hamptoni* from Myanmar prove to be greatly distinct from populations in the eastern part of species range, the widely distributed red-eyed *Pareas* with smooth dorsals from Taiwan, China and South-east Asia can be regarded as full species *P. formosensis*, while the extent of distribution of this species will need a more thorough review. Unfortunately, we failed to obtain the topotype material from Myanmar and new samples from this country are unlikely to be available in the near future.

Psammodynastes compressus Oshima 1910 is synonym of *P. formosensis*

In 1910, Masamitsu Oshima provided a brief description of a new species *Psammodynastes compressus*, known from a single specimen collected in 'Kokwangai, Taihoku'. Later, Oshima (1916) himself invalidated *P. compressus* as a junior synonym of *Amblycephalus formosensis*. Our study showed that two forms of *Pareas* can be found on the territory of the former Taihoku Prefecture: the red-eyed form inhabiting the southernmost part and the yellow-eyed form 2 distributed more widely within the range of Taipei and New Taipei City. Thus, for evaluation of taxonomic status of Taiwanese *Pareas*, more detailed information on taxonomic assignation of *Psammodynastes compressus* Oshima 1910 is needed.

The single specimen of pareatid snake, which was collected by Masamitsu Oshima from 'Taihoku, Taiwan', is now tagged as *Pareas formosensis* (NSMT H02567) preserved in National Museum of Nature and Science, Tsukuba, Japan. A careful examination of this specimen indicated remarkable similarities with counts, measurements and descriptions provided by Oshima in his original paper (1910). The NSMT H02567 specimen shows the following morphological character states (data from Oshima 1910 given in brackets): IL 7 [5]; VEN 182 [182]; SC 75 [75]; TL 60.50 [60.80] cm; TaL 11.40 [13.50] cm; HL 16.39 [N/A] mm; SnL 4.27 [N/A] mm. Slight differences in measurements could be explained by the long preservation time of the specimen in alcohol. Difference in numbers of infralabials is likely caused by alternative methods of calculation: Oshima gives no details on counting method he used and no figure of head scalation of the new species; however, the IL count he reports as 5 is never observed in the genus *Pareas* (Guo & Deng 2009); obviously Oshima did not include two posterior elongated infralabials in his count. However, precise match of ventral and subcaudal counts, as well as temporal region scalation, indicates that Oshima likely made his 1910 description based on this specimen. NSMT H02567 has entirely smooth dorsal scales; according to the results of our multivariate analyses, it undoubtedly belongs in the red-eyed clade of Taiwanese *Pareas* (Fig. 3). We redefine the geographic locality 'Kokwangai' as environs of Ankeng, Xindian District (Taihoku Administrative Office 1919), where both red-eyed and yellow-eyed forms of *Pareas* can be found today. Therefore, we conclude that specimen NSMT H02567 is the holotype of *Psammodynastes compressus* Oshima 1910; the name appears to be a junior synonym of *P. formosensis* (Van Denburgh 1909) *sensu stricto*.

The yellowed-eyed form of Pareas contains two valid species

In their review of East Asian *Pareas*, Ota *et al.* (1997b) examined material collected from Taiwan and Japanese islands of Iriomote and Ishigaki (Okinawa, Yaeyama group) and concluded that *P. komaii* (Maki 1931) should be regarded as a junior synonym of *P. formosensis* (Van Denburgh 1909). This taxonomic revision was based on their examination of preserved specimens, including holotypes of *P. komaii* (Maki 1931) and *P. formosensis* (Van Denburgh 1909). However, they did not examine living specimens for characterization of iris coloration. As snakes with smooth and keeled dorsals occur in some areas and are often found sympatrically, they interpreted that snakes with keeled or smooth scales represent intraspecific variation within *P. formosensis* (Van Denburgh 1909). Our PCA and DA demonstrated that both the holotype and the paratype of *P. komaii* (Maki 1931) were assigned to the yellow-eyed form 1 (Fig. 3). In contrary to Ota *et al.* (1997b), our morphological and molecular data suggest that *P. komaii* should be restored as a valid name. This species can be easily distinguished from *P. formosensis* by its yellow iris and strongly keeled dorsals.

The third clade in Taiwan represents snakes with yellow iris and weakly keeled dorsals (yellow-eyed form 2). A small proportion of *P. iwasakii* represent shared c-mos haplotype that was found in these snakes, indicating the comparatively shorter separation history between these two closely related species. However, owing to a relatively large mitochondrial sequence divergence, as well as diagnostic morphological

characters (a more elongated head and significantly higher numbers of infralabials, ventrals and subcaudals in *P. iwasakii*; see Table 1), we suggest the yellow-eyed form 2 should be evaluated as a new species which we describe below.

Species diversity of Pareas remains to be uncovered in the future

Based on the literature data, Jiang (2004b) proposed that *P. chinensis* (Barbour 1912) was a synonym of *P. formosensis* (Van Denburgh 1909). However, this decision was tentatively made without referring to any certain specimens. To clarify this problem, Guo *et al.* (2011) used four *Pareas* tissues from our collection in Taiwan and rejected Jiang's rearrangement based on molecular phylogenetic data. However, the taxonomy of Guo *et al.* (2011) is incomplete, as their collection lacks the real *P. formosensis sensu stricto* (the red-eyed form). According to our phylogenetic tree (Fig. 2A), the four '*P. formosensis*' individuals they used were assigned to either *P. komaii* (JF827687) or the new *Pareas* species (JF827685, JF827686, JF827688). The validity of *P. chinensis* is still supported in our study; while the additional material from Taiwan hinted the under-estimation of pareatid diversity in East Asia.

Our study also uncovered the distribution pattern of the three Taiwanese pareatids. *Pareas formosensis* is distributed throughout the whole mountain regions except for the north-eastern tip of the island. Across this area, one other species, either the yellow-eyed form 1 (*P. komaii*) or the yellow-eyed form 2 (*Pareas* sp. nov.), coexists with *P. formosensis* (Fig. 1). *Pareas komaii* and the nominal new species occupy central-southern and northern Taiwan, respectively. The ranges of the three clades overlap in central Taiwan; however, we have not found any evidence of hybridization.

The speciation of *Pareas* in Taiwan might be attributed to two probable factors: the complicated geological history of the island and the evolution of their asymmetric dentition. The repetitive connection and separation among island groups between Taiwan, Ryukyu and mainland Asia has contributed to species or genetic differentiation in this region, which has been widely discussed in the literature (Lin *et al.* 2002; Tseng *et al.* 2014). In our samples, *P. komaii* (the yellow-eyed form 1) has shown significant genetic differentiation between eastern and western populations, congruent to the patterns discovered in vipers (Creer *et al.* 2001), cobras (Lin *et al.* 2008) and tree frogs (Lin *et al.* 2012). On the other hand, studies on the asymmetric mandibular teeth of *Pareas* snakes and their mollusc prey have highlighted a novel aspect on the evolution of these snakes. Although the sample size is limited, preliminary evaluation on dentition asymmetric index showed substantial variation among the specimens which we evaluated in this study (Table S3). Further studies of correlation between dentition asymmetry and their prey preference with higher sample size will give insight into dietary resource partitioning and niche differentiation between these species.

Species description

Pareas atayal *sp. nov*.

Holotype. NMNS 05594 (Fig. S3), adult male collected by Chung-Wei You on August 27th, 2009 from TAIWAN, Taoyuan County, Fuxing Township, Sileng (24.653570 N, 121.409266 E) with elevation *ca.* 925 m.

Paratypes. NMNS 05584, 05585, 05586, 05587, 05588, 05589, 05591, 05593, 05595, 05596; ZMMU R-14434, R-14435 and R-14436. All the paratypes collected during 2009–2013 by Chung-Wei You, Jia-Wei Lin and Ren-Jay Wang in northern Taiwan.

Other material. NMNS 05590, 05592, 05597 collected during 2009–2011 by Jia-Wei Lin and Chung-Wei You in northern Taiwan.

Etymology. The new species is named with reference to its distribution which is similar to the native Taiwan aboriginal people, the Atayal, inhabiting mountain regions of northern Taiwan. Common name in English: '*Atayal Slug-eating Snake*'.

Diagnosis. *Pareas atayal* sp. nov. is a small (about 50 cm) slender yellow-brown snake, a member of *Pareas hamptoni* group on the basis of the following combination of morphological attributes: (1) nasal simple, not divided; (2) loreal not contacting the eye; (3) prefrontal contacting the eye; (4) one pre-ocular; (5) subocular single, crescent-shaped; (6) two anterior temporals, three to four posterior temporals (2 + 4); (7) slightly enlarged median vertebral and two adjacent rows of scales. *Pareas atayal* sp. nov. differs from all other members of the *Pareas* by the combination of the following morphological characters: (8) tail comprising 22% of the TL; (9) 7–9 infralabial scales; (10) 15 dorsal scale rows slightly keeled in seven rows at mid-body; dorsal scales smooth or one row slightly keeled in the anterior 1/4 of TL; (11) head notably elongated with HW/HL ratio 28%; (12) 174–188 ventrals without lateral keels; (13) 71–77 divided subcaudals; (14) iris colour bright yellow to light orange; (15) 50 slightly billowing vertical dark bars on the trunk (the bars about 1–2 scales wide); (16) two very clear thin black postorbital stripes beginning from lower and upper edges of each postorbital scale, with lower postorbital stripe reaching the anterior part of SL7, not continuing to the lower jaw and chin; the left and right upper postorbital stripes forming a bifurcation at the base

of the head forming an M-shaped figure (about 4–6 scale-length) and often connecting together behind head; (17) 6–7 maxillary teeth; 11–13 functional teeth on the left mandible and 19–20 on the right.

Description of holotype. The holotype (Fig. S3) is an adult female with body slender and notably flattened laterally (425.5 mm SVL; 132.0 mm TaL; 560.0 mm TL); head comparatively small (17.7 mm HL; 11.4 mm HW; 6.9 mm HH; HL/SVL ratio 4.2%), narrowly elongated, distinctly compressed laterally and oval in dorsal view (HW/HL ratio 27%), clearly distinct from neck; vertebral ridge poorly developed; snout blunt, widely spatulate (4.0 mm SnL; 2.6 mm EN); eye very large (2.9 mm ED; 5.2 mm IO), about 0.17 times the head length, rounded in shape and notably protuberant; pupil vertical; tail slightly laterally compressed at the basis, oval-shaped in cross section in the middle of length and round in the posterior 1/3, ending in an acuminated tail cap (TaL/TL ratio 24%).

Dentition. Maxillary teeth: six functional teeth on the left side and seven on the right side. Mandibular teeth: 11 functional teeth on the left lower jaw and 20 on the right (Fig. S2).

Head scalation. In dorsal view (Fig. S4B): one rostral, large, slightly wider than high; two internasals, much wider than long; two prefrontals, large, pentagonal, almost as long as wide; two supraoculars, pentagonal, elongated; one frontal, large, subhexagonal; and two parietals, irregularly trapezoid in shape, about twice as large as frontal; no enlarged nuchal scales present. In lateral view (Fig. S4A): nasal 1/1, pierced by a large crescent-shape nostril; squarish loreal scale 1/1, not contacting eye; pre-oculars 1/1, in contact with eye; no presubocular; 7/7 supralabials increasing in size from front to back, separated from eye by crescent-shaped subocular scale; postocular distinct, not fused with subocular, in contact with eye; distance between eye and snout tip (snout length) 1.4 times eye diameter; pupil vertical and slightly elliptical; temporals 2 + 4/2 + 4. In ventral view (Fig. S4C): mental triangular, fully separating first pair of infralabials; infralabials 9/9 (in ventral view only seven pairs apparent); three pairs of chin shields interlaced, no mental groove under chin and throat.

Body scalation. Dorsal scales in 15 rows along whole body, DSR formula: 15–15–15; on neck (approximately one HL from the head basis) median three rows (vertebral scale row and two lateral rows) feebly keeled, at middle of body length (VEN92–VEN93) seven dorsal scale rows notably keeled; at posterior third of body length (approximately one HL to the vent) nine dorsal scale rows notably keeled; vertebral scales slightly enlarged (one medial row); ventrals VEN 185, with rounded outer margins, without lateral keels; anal plate entire, crescent in shape; subcaudals SC 76 (excluding terminal spine), all divided/paired; terminal caudal scale forming acuminated tail cap.

Natural history notes. *Pareas atayal* inhabits various types of forests at altitudes of *ca.* 100–2000 m above sea level. The new species feeds on a variety of land snails and slugs; strictly nocturnal, mostly active after twilight around 20:00.

Distribution. The new species is endemic to Taiwan. To date, *Pareas atayal* is confined to Taipei and New Taipei City, Yilan, Taoyuan, Hsinchu and Nantou counties of Taiwan.

Comparisons. For comparisons of the new species with other congeners, see Table 1 and Table S4. For the full species description, see Appendix S1.

Acknowledgements

We are grateful to the assistance from M. Hoso, who provided us valuable comments during this research, as well as the production of the dentition X-ray tomography figure. We kindly thank H. Ota for his kind support, and S. Kawada for permanent support and permission to examine specimens in the National Museum of Nature and Science (NSMT), Tsukuba, Japan, and to H. Nagaoka and N. Kurihara for all their assistance. Special gratitude to S. Shimoinaba (NSMT) for her kind helps with finding old literature and old maps of Taiwan, and J.-W. Lin for his support on a large number of samples from the wild and providing original unpublished data on ecology of Taiwanese Pareas. We are also grateful for our colleagues and friends: S.-H. Yen, Y.-P. Lin, S.-P. Tseng, R.-J. Wang, H.-Y. Tseng, N. B. Ananjeva, E. A. Galoyan, L. P. Korzoun, L. X. Son, D. H. Nguyen, N. L. Orlov, I. V. Palko, E. N. Solovyeva, A. B. Vassilieva, V. Yashin, K. Ishihara, T. T. Kusuonki and D. Horiguchi for their continued support and helps during the fieldwork and in the laboratory. We are grateful to S. Shonleben for help with proofreading of the manuscript and useful comments. We are sincerely grateful to the editor and two anonymous reviewers who provided useful comments which helped us to improve the previous version of the manuscript. This work was supported by Ministry of Science and Technology, Taiwan (NSC 103-2923-B-003-001-MY3), specimen collection, preservation and examination was completed with financial support from Russian Science Foundation (RSF grant Nº 14-50-00029), the study was partially supported by the Russian Foundation of Basic Research (Grants No. RFBR 15-04-08393 and RFBR Taiwan No. 14-04-92000), and by a Grant of the President of Russian Federation (MK-5815.2014.4).

References

Barbour, T. (1912). Amphibia and Reptilia. *Memoirs of the Museum of Comparative Zoology*, *40*, 125–136.

Boulenger, G. A. (1905). Descriptions of two new snakes from upper Burma. *Journal of the Bombay Natural History Society*, *16*, 235–237.

Cox, M. J., van Dijk, P. P., Nabhitabhata, J. & Thirakhupt, K. (1998). *A Photographic Guide to Snakes and Other Reptiles of Peninsular Malaysia, Singapore and Thailand*. London: New Holland Publishing.

Creer, S., Malhotra, A., Thorpe, R. S. & Chou, W.-H. (2001). Multiple causation of phylogeographical pattern as revealed by nested clade analysis of the bamboo viper (Trimeresurus stejnegeri) within Taiwan. *Molecular Ecology*, *10*, 1967–1981.

Das, I. (2010). *A Field Guide to the Reptiles of South-East Asia*. London: New Holland Publishing.

De Queiroz, A., Lawson, R. & Lemos-Espinal, J. A. (2002). Phylogenetic relationships of North American garter snakes (*Thamnophis*) based on four mitochondrial genes: how much DNA is enough? *Molecular Phylogenetics and Evolution*, *22*, 315–329.

Ding, L., Gan, X. N., He, S. P. & Zhao, E. M. (2011). A phylogeographic, demographic and historical analysis of the short-tailed pit viper (*Gloydius brevicaudus*): evidence for early divergence and late expansion during the Pleistocene. *Molecular Ecology*, *20*, 1905–1922.

Dowling, H. G. (1951). A proposed standard system of counting ventral in snakes. *Journal of Herpetology*, *1*, 97–99.

Grossmann, W. & Tillack, F. (2003). On the taxonomic status of *Asthenodipsas tropidonotus* (Van Lidth de Jeude, 1923) and *Pareas vertebralis* (Boulenger, 1900) (Serpentes: Colubridae: Pareatinae). *Russian Journal of Herpetology*, *10*, 175–190.

Guo, K. J. & Deng, X. J. (2009). A new species of *Pareas* (Serpentes: Colubridae: Pareatinae) from the Gaoligong Mountains, southwestern China. *Zootaxa*, *2008*, 53–60.

Guo, Y. H., Wu, Y. K., He, S. P., Shi, H. T. & Zhao, E. M. (2011). Systematics and molecular of Asian snail-eating snakes (Pareatidae). *Zootaza*, *3001*, 57–64.

Hoso, M. (2007). Oviposition and hatchling diet of a snail-eating snake *Pareas iwasakii* (Colubridae: Pareatinae). *Current Herpetology*, *26*, 41–43.

Hoso, M. & Hori, M. (2006). Identification of molluscan prey from feces of Iwasaki's slug snake, *Pareas iwasakii*. *Herpetological Review*, *37*, 174–176.

Hoso, M. & Hori, M. (2008). Divergent shell shape as an antipredator adaptation in tropical land snails. *The American Naturalist*, *172*, 726–732.

Hoso, M., Asami, T. & Hori, M. (2007). Right-handed snakes: convergent evolution of asymmetry for functional specialization. *Biology Letters*, *3*, 169–172.

Hoso, M., Kameda, Y., Wu, S. P., Asami, T., Kato, M. & Hori, M. (2010). A speciation gene for left–right reversal in snails results in anti-predator adaptation. *Nature Communications*, *1*, 133.

Huang, Q. Y. (2004). *Pareas chinensis* (Barbour, 1912) should be a junior synonym of *Pareas formosensis* (Van Denburgh, 1909). *Sichuan Journal of Zoology*, *23*, 209–210.

International Commission on Zoological Nomenclature (ICZN) (1971). Opinion 963. *Amblycephalus* Kuhl & van Hasselt, 1822 (Reptilia): suppressed under the Plenary Powers. *Bulletin of Zoological Nomenclature*, *28*, 44–45.

Jiang, Y.-M. (2004a). *Pareas macularius* Theobald, 1868 should be a junior synonym of *Pareas margaritophorus* (Jan, 1866). *Sichuan Journal of Zoology*, *23*, 207–208 [in Chinese].

Jiang, Y.-M. (2004b). *Pareas chinensis* (Barbour, 1912) should be a junior synonym of *Pareas formosensis* (Van Denburgh, 1909). *Sichuan Journal of Zoology*, *23*, 209–210 [in Chinese].

Keogh, J. S. (1999). Evolutionary implications of hemipenial morphology in the terrestrial Australian elapid snakes. *Zoological Journal of the Linnean Society*, *125*, 239–278.

Lanfear, R., Calcott, B., Ho, S. Y. & Guindon, S. (2012). PartitionFinder: combined selection of partitioning schemes and substitution models for phylogenetic analyses. *Molecular Biology and Evolution*, *29*, 1695–1701.

Lawson, R., Slowinski, J. B., Crother, B. I. & Burbrink, F. T. (2005). Phylogeny of the Colubroidea (Serpentes): new evidence from mitochondrial and nuclear genes. *Molecular Phylogenetics and Evolution*, *37*, 581–601.

Librado, P. & Rozas, J. (2009). DnaSP v5: A software for comprehensive analysis of DNA polymorphism data. *Bioinformatics*, *25*, 1451–1452.

Lin, C.-W. (2010). *Terrestrial Molluscs Mucus Trailing Behavior of Taiwan Slug Snake*, Pareas formosensis. Master thesis, Department of Life Science, National Taiwan Normal University [in Chinese].

Lin, S.-M., Chen, C. A. & Lue, K.-Y. (2002). Molecular phylogeny and biogeography of the grass lizards genus *Takydromus* (Reptilia: Lacertidae) of East Asia. *Molecular Phylogenetics and Evolution*, *22*, 276–288.

Lin, H.-C., Li, S.-H., Fong, J. & Lin, S.-M. (2008). Ventral coloration differentiation and mitochondrial sequences of the Chinese Cobra (*Naja atra*) in Taiwan. *Conservation Genetics*, *9*, 1089–1097.

Lin, H.-D., Chen, Y.-R. & Lin, S.-M. (2012). Strict consistency between genetic and topographic landscapes of the brown tree frog (*Buergeria robusta*) in Taiwan. *Molecular Phylogenetics and Evolution*, *62*, 251–262.

Lue, K. Y. (1989). *Taiwan Snakes*. Taipei County: Taiwan Provincial Government, Department of Education [in Chinese].

Maki, M. (1931). *A Monograph of the Snakes of Japan*. Tokyo: Dai-Ichi Shobo.

Manthey, U. & Grossmann, W. (1997). *Amphibien & Reptilien Südostasiens*. Münster: Natur und Tier Verlag.

Nakamura, K. & Uéno, S.-I. (1963). *Japanese Reptiles and Amphibians in Colour*. Osaka: Hoikusha Publishing Co. Ltd.

Nguyen, V. S., Ho, T. C. & Nguyen, Q. T. (2009). *Herpetofauna of Vietnam*. Frankfurt: Edition Chimaira.

Orlov, N. L., Murphy, R. W. & Papenfuss, T. J. (2000). List of snakes of Tam-Dao mountain ridge (Tonkin, Vietnam). *Russian Journal of Herpetology*, 7, 69–80.

Oshima, M. (1910). An annotated list of Formosan snakes, with descriptions of four new species and one new subspecies. *Annotations Zoologicae Japonensis*, 7, 185–207.

Oshima, M. (1916). A correction of scientific species names of Taiwanese snakes. *Zoological Magazine*, *28*, 84–86 [in Japanese].

Ota, H., Bogadek, A. & Lau, M. W. (1997a). Comments on the taxonomic status of the montane *Pareas* from Hong Kong (Squamata: Colubridae). *Journal of the Taiwan Museum*, *50*, 85–91.

Ota, H., Lin, J.-T., Hirata, T. & Chen, S.-L. (1997b). Systematic review of colubrid snakes of the genus *Pareas* in the East Asian Islands. *Journal of Herpetology*, *31*, 79–87.

Pope, C. H. (1935). *The Reptiles of China. Turtles, Crocodilians, Snakes, Lizards. Natural History of Central Asia Vol. X*. New York: The American Museum of Natural History.

Pyron, R. A., Burbrink, F. T., Colli, G. R., de Oca, A. N. M., Vitt, L. J., Kuczynski, C. A. & Wiens, J. J. (2011). The phylogeny of advanced snakes (Colubroidea), with discovery of a new subfamily and comparison of support methods for likelihood trees. *Molecular Phylogenetics and Evolution*, *58*, 329–342.

Rambaut, A. & Drummond, A. (2009). Tracer v1. 5: an MCMC trace analysis tool. Available from, http://tree.bio.ed.ac.uk/software/tracer/. Edinburgh: Institute of Evolutionary Biology, University of Edinburgh.

Rao, D. Q. & Yang, D. T. (1992). Phylogenetic systematics of Pareatinae (Serpentes) of Southeastern Asia and adjacent islands with relationship between it and the geology changes. *Acta Zoologica Sinica*, *38*, 139–150 [in Chinese].

Ronquist, F., Teslenko, M., van der Mark, P., Ayres, D. L., Darling, A., Höhna, S., Larget, B., Liu, L., Suchard, M. A. & Huelsenbeck, J. P. (2012). MrBayes 3.2: Efficient Bayesian phylogenetic inference and model choice across a large model space. *Systematic Biology*, *51*, 539–542.

Slowinski, J. B. & Lawson, R. (2002). Snake phylogeny: evidence from nuclear and mitochondrial genes. *Molecular Phylogenetics and Evolution*, *23*, 194–202.

Smith, M. A. (1943). *The Fauna of British India Ceylon and Burma, Including the Whole of the Indo-Chinese Sub-Region. Reptilia and Amphibia. Vol. III. Serpentes*. London: Taylor & Francis Group.

Sotka, E. E., Wares, J. P., Barth, J. A., Grosberg, R. K. & Palumbi, S. R. (2004). Strong genetic clines and geographical variation in gene flow in the rocky intertidal barnacle *Balanus glandula*. *Molecular Ecology*, *13*, 2143–2156.

Stamatakis, A. (2006). RAxML-VI-HPC: maximum likelihood-based phylogenetic analyses with thousands of taxa and mixed models. *Bioinformatics*, *22*, 2688–2690.

Stephens, M. & Scheet, P. (2005). Accounting for decay of linkage disequilibrium in haplotype inference and missing data imputation. *American Journal of Human Genetics*, *76*, 449–462.

Stephens, M., Smith, N. J. & Donnelly, P. (2001). A new statistical method for haplotype reconstruction from population data. *American Journal of Human Genetics*, *68*, 978–989.

Stuebing, R. B., Inger, R. F. & Tan, F. L. (1999). *A Field Guide to the Snakes of Borneo*. Kota Kinabalu: Natural History Publications (Borneo).

Taihoku Administrative Office (1919). *Topography of Taihoku Prefecture (Taihoku-Chou Shi)*. Taihoku: Taiwan Ichi-nichi Shinpousha, 729 p.

Tamura, K., Stecher, G., Peterson, D., Filipski, A. & Kumar, S. (2013). MEGA6: Molecular Evolutionary Genetics Analysis Version 6.0. *Molecular Biology and Evolution*, *30*, 2725–2729.

Taylor, E. H. (1965). The serpents of Thailand and adjacent waters. *University of Kansas Science Bulletin*, *45*, 609–1096.

Tseng, S.-P., Li, S.-H., Hsieh, C.-H., Wang, H.-Y. & Lin, S.-M. (2014). Influence of gene flow on divergence dating – implications for the speciation history of *Takydromus* grass lizards. *Molecular Ecology*, *23*, 4770–4784.

Van Denburgh, J. (1909). New and previously unrecorded species of reptiles and amphibians from the island of Formosa. *Proceedings of the California Academy of Sciences*, *3*, 49–56.

Vassilieva, A. B., Geissler, P., Galoyan, E. A., Poyarkov, N. A., Jr, Van Devender, R. W. & Böhme, W. (2013). A new species of Kukri Snake (Oligodon Fitzinger, 1826; Squamata: Colubridae) from the Cat Tien National Park, southern Vietnam. *Zootaxa*, *3702*, 233–246.

Vermeij, G. J. (1975). Evolution and distribution of left-handed and planispiral coiling in snails. *Nature*, *254*, 419–420.

Vidal, N., Delmas, A.-S., David, P., Cruaud, C., Couloux, A. & Hedges, S. B. (2007). The phylogeny and classification of caenophidian snakes inferred from seven nuclear protein-coding genes. *Comptes rendus biologies*, *330*, 182–187.

Williams, K. L. & Wallach, V. (1989). *Snakes of the World. Vol. 1. Synopsis of Snake Generic Names*. Malabar: R. E. Krieger Publishing Company.

Zaher, H., Grazziotin, F. G., Cadle, J. E., Murphy, R. W., Moura-Leite, J. C. D. & Bonatto, S. L. (2009). Molecular phylogeny of advanced snakes (Serpentes, Caenophidia) with an emphasis on South American Xenodontines: a revised classification and descriptions of new taxa. *Papéis Avulsos de Zoologia (São Paulo)*, *49*, 115–153.

Zhao, E.-M., Huang, M.-H. & Zong, Y. (Eds). (1998). *Fauna Sinica Reptilia Vol. 3, Squamata: Serpentes*. Beijing: Science Press [in Chinese].

Supporting Information

Additional Supporting Information may be found in the online version of this article:

Appendix S1. Species description of *Pareas atayal* sp. nov. in full details.

Table S1. Sample IDs, original and revised identification of species, sample locality, GenBank accession number, and source of specimens used in this study.

Table S2. Between-species divergence and within-species polymorphism among *Pareas* spp. from mitochondrial cytochrome *b* sequences.

Table S3. Mandibular teeth count and asymmetry index for *Pareas atayal* sp. nov., *P. formosensis* and *P. komaii*.

Table S4. Diagnostic features of scalation and color pattern of currently recognized species of *Pareas*.

Fig. S1. Lateral and dorsal views of a yellow-eyed *Pareas* and a red-eyed *Pareas* with identical body length.

Fig. S2. Volume reconstruction of high-resolution X-ray computed tomography data showing cranium and mandibles of the holotype of *Pareas atayal* sp. nov.

Fig. S3. Dorsal and ventral view of the holotype of *Pareas atayal* sp. nov.

Fig. S4. Head scalation of the holotype of *Pareas atayal* sp. nov.

Fig. S5. Hemipenial sructures of the paratype of *Pareas atayal* sp. nov.

Supplementary Information

Title: Diversity of the snail-eating snakes *Pareas* (Serpentes, Pareatidae) from Taiwan

Authors: Chung-Wei You[1], Nikolay A. Poyarkov, Jr.[2,3], Si-Min Lin[1*]

[1] Department of Life Science, National Taiwan Normal University

[2] Department of Vertebrate Zoology, Biological Faculty, Lomonosov Moscow State University

[3] Joint Russian-Vietnamese Tropical Research and Technological Center, South Branch, Vietnam

[*] Corresponding author: fish@ntnu.edu.tw; fishdna@ms31.hinet.net

Species description (the full version)

***Pareas atayal* sp. nov.**

Holotype. NMNS 05594 (Supplementary Fig. S3), adult male collected by Chung-Wei You on August 27th, 2009 from TAIWAN, Taoyuan County, Fuxing Township, Sileng (24.653570 N, 121.409266 E) with elevation ca. 925 m. The snake was found climbing on a tree branch beside the road; the surrounding environment is moist hardwood forest.

Paratypes. NMNS 05584, 05585, 05586, collected from TAIWAN, Taipei City, Datun Mountain; NMNS 05587 from New Taipei City, Shiding; NMNS 05588 from New Taipei City, Sanxia; NMNS 05589 and 05591 from New Taipei City, Wulai; NMNS 05593 and 05595 from Taoyuan County, Fuxing township; NMNS 05596 from Nantou County, Xitou. All the above 10 specimens were collected during 2009–2010 by Jia-Wei Lin and Chung-Wei You and are now preserved in National Museum of Natural Science (NMNS), Taichung, Taiwan. ZMMU R-14434, R-14435, and R-14436 from TAIWAN, Taoyuan County, Fuxing township; collected during 2010–2013 by Ren-Jay Wang and Chung-Wei You, are now preserved in Zoological Museum of Moscow State University (ZMMU), Moscow, Russian Federation. All the snakes were found either on forest road sides, or at the edge of the forest. The surrounding

environment was lowland moist hardwood forest or secondary forest.

Other material. NMNS 05590 from TAIWAN, New Taipei City, Wulai; NMNS 05592 from Taoyuan County, Fuxing township; NMNS 05597 from Nantou County, Xitou; all specimens collected during 2009–2011 by Jia-Wei Lin and Chung-Wei You and are preserved in National Museum of Natural Science (NMNS), Taichung, Taiwan.

Etymology. The specific epithet of the new species "*atayal*" is a Latinized noun in apposition and is invariable. The new species is named with reference to its distribution which is similar to the native Taiwan aboriginal people, the Atayal, inhabiting mountain regions of northern Taiwan. We suggest the following common names: "*Atayal Slug-eating Snake*" in English and "*Tai-Ya Dun-Tou-She*" in Chinese.

Diagnosis.

Pareas atayal sp. nov. is a small (about 50 cm) slender yellow-brown snake, a member of *Pareas hamptoni* group on the basis of the following combination of morphological attributes: (1) nasal simple, not divided; (2) loreal not contacting the eye; (3) prefrontal contacting the eye; (4) one preocular; (5) subocular single, crescent-shaped; (6) two anterior temporals, three to four posterior temporals (2+4); (7) slightly enlarged median vertebral and two adjacent rows of scales. *Pareas atayal* sp. nov. differs from all other members of the *Pareas* by the combination of the following morphological characters: (8) tail comprising 22% of the TL; (9) 7 to 9 infralabial scales; (10) 15 dorsal scale rows slightly keeled in 7 rows at midbody; dorsal scales smooth or 1 row slightly keeled in the anterior 1/4 of TL; (11) head notably elongated with HW/HL ratio 28%; (12) 174–188 ventrals without lateral keels; (13) 71–77 divided subcaudals; (14) iris color bright yellow to light orange; (15) 50 slightly billowing vertical dark bars on the trunk (the bars about 1–2 scales wide); (16) two very clear thin black postorbital stripes beginning from lower and upper edges of each postorbital scale, with lower postorbital stripe reaching the anterior part of SL7, not continuing to the lower jaw

and chin; the left and right upper postorbital stripes forming a bifurcation at the base of the head forming an M-shaped figure (about 4–6 scale-length) and often connecting together behind head; (17) 6–7 maxillary teeth; 11–13 functional teeth on the left mandible and 19–20 on the right.

Description of holotype.

The holotype (Supplementary Fig. S3) is an adult female with body slender and notably flattened laterally (425.5 mm SVL; 132.0 mm TaL; 560.0 mm TL); head comparatively small (17.7 mm HL; 11.4 mm HW; 6.9 mm HH; HL/SVL ratio 4.2%), narrowly elongated, distinctly compressed laterally and oval in dorsal view (HW/HL ratio 27%), clearly distinct from thin neck (head more than two times wider than neck width near the head basis); vertebral ridge poorly developed; snout blunt, widely spatulate in form (4.0 mm SnL; 2.6 mm EN); lower mouth with snout clearly projecting over the lower jaw; rostral scale possessing large concave furrow on ventral surface; large slightly crescent-shaped nostril piercing located in the center of the posterior half of single nasal, 4.4 mm IN; eye very large (2.9 mm ED; 5.2 mm IO), about 0.17 times the head length, rounded in shape and notably protuberant; pupil vertical; tail rather short (TaL/TL ratio 24%), slightly laterally compressed at the basis, oval-shaped in cross-section in the middle of length and round in cross-section in the posterior 1/3 of length, ending in an acuminated tail cap.

Dentition. Maxillary teeth: 6 functional teeth on the left side and 7 on the right. Palatine dentition well developed. Mandibular teeth: 11 functional teeth on the left lower jaw and 20 on the right (Supplementary Fig. S2). Anterior mandibular teeth strongly enlarged, blade-like, gradually decreasing in size in posterior direction; the most posterior part of the tooth row of the left mandible flattened with no teeth recognizable.

Head scalation. In dorsal view (Supplementary Fig. S4B): 1 rostral scale, 2 internasals, 2 prefrontals, 2 supraoculars, 1 frontal, and 2 parietals. Rostral large, slightly wider than high

(height/width ratio 0.92), just reaching upper surface of snout, with large concave furrow on the ventral side; internasals much wider than long (width/length ratio 2.10), narrowing and slightly curving back laterally (in dorsal view), anteriorly in contact with rostral, laterally in contact with nasal and loreal, posteriorly in contact with prefrontal, not contacting preocular; prefrontals large, pentagonal, almost as long as wide (length/width ratio 1.06), laterally in contact with loreal and preocular, posteriorly in contact with eye, supraorbital and frontal; internasal suture shorter than prefrontal suture (ratio 0.46); supraoculars pentagonal, elongated, about 1.76 times longer than wide in dorsal view; supraocular in contact with prefrontal, frontal, parietal and postocular; frontal large, sub-hexagonal, with acute anterior and rounded posterior angles, about 1.16 times longer than wide, frontal 1.6 times longer than its distance from tip of snout; parietals large, irregularly trapezoid in shape, about twice as large as frontal, about 1.71 times longer than broad, median parietal suture about as long as frontal (length ratio 1.06), anteriorly contacting frontal and supraocular, laterally contacting postorbital, upper anterior and posterior temporals, bordered posteriorly by 7 scales on the left side and by 6 scales on the right side (including the temporals); no enlarged nuchal scales present. In lateral view (Supplementary Fig. S4A): 1/1 entire, simple, slightly elongated nasal, ovoid in shape (1.30 times longer than wide), pierced by a large crescent-shape nostril, located in the center of the posterior half of nasal, nostril horizontal diameter ca. 3.6 times shorter than nasal length; 1/1 squarish loreal scale, almost semicircular with anterior edge slightly concave, about 1.13 times broader than deep, not contacting eye, contacting second supralabial, subocular and preorbital scales laterally and posteriorly; preoculars 1/1, trapezoid, in contact with eye, prefrontal, loreal and subocular, about 1.40 times deeper than broad; no presubocular; 7/7 supralabials squarish in form, increasing in size from front to back, separated from eye by crescent-shaped subocular scale, SL-I in contact with nasal, SL-II in contact with nasal, loreal and subocular, notably higher than SL-I (around 1.45 times), SL-III and SL-IV notably lower than SL-II (around 1.59 times) and contact subocular, SL-V higher

than SL-III and SL-IV (around 1.48 times) and in contact with subocular and lower anterior temporal, forming a sharp angle, SL-VI in contact with lower anterior and posterior temporals, SL-VII (largest) in contact with lower posterior temporal and postemporal scale; SL-VI and SL-VII being strongly enlarged and elongated (length/height ratios around 2.29 and 3.53 respectively); 1/1 suboculars semi-crescent in shape, edging the lower 1/3 of eye diameter, also in contact with preocular, loreal, suboculars SL-II–SL-V, lower anterior temporal and postocular scales, anterior portion of subocular widened and axe-shaped; postocular distinct, not fused with subocular, semicircular in shape, in contact with eye, supraocular, parietal, upper and lower anterior temporals, and subocular; distance between eye and snout tip (snout length) 1.4 times eye diameter; pupil vertical and slightly elliptical; temporals 2+4/2+4, upper anterior one almost quadrangular, elongated (length/height ratio around 2.08) on both sides, lower anterior temporal enlarged, sub-hexagonal in shape, ca. 1.7 times longer than high, around 1.3 times bigger than upper anterior temporal; upper posterior temporal on left side of head pentagonal, approximately equal to the upper anterior, elongated, slightly tapering posteriorly, second posterior temporal quadrangular, larger than upper anterior, elongated and contacting upper anterior temporal with very short vertical suture; third posterior the smallest, rhomboid, ca. 1.7x smaller than the upper anterior temporal, lower posterior temporal pentagonal, elongated, the largest, 1.42 times longer than upper anterior temporal; on right side upper posterior temporal smallest, ca. 2.5 times smaller than second posterior temporal, rhomboid, second and third posterior temporals roughly same size, pentagonal, elongated, lower posterior temporal largest. In ventral view (Supplementary Fig. S4C): mental triangular, 3.0 times broader than long, fully separating first pair of infralabials; 9/9 infralabials (in ventral view only 7 pairs apparent): anterior-most IL-I not in contact with opposite along midline, but in contact with mental and with first pair of chin shields, IL-I to IL-IV in contact with first pair of slightly enlarged chin shields, IL-IV to IL-V in contact with somewhat smaller second pair of chin shields, IL-V to IL-VII on left side and IL-V to IL-VI on right side

in contact with third pair of chin shields; 3 pairs of chin shields interlaced, no mental groove under chin and throat; anterior chin shields relatively large, much longer than broad (length/width ratio around 1.8), followed by two pairs of chin shields much broader than long posteriorly; preventral scale one small asymmetric triangular scale on the left side.

Body scalation. Dorsal scales in 15 rows along whole body, DSR formula: 15-15-15; on neck (approximately one HL from the head basis) median 3 rows (vertebral scale row and two lateral rows) feebly keeled, at middle of body length (VEN92–VEN93) 7 dorsal scale rows notably keeled; at posterior third of body length (approximately 1 HL to the vent) 9 dorsal scale rows notably keeled, at mid-dorsum to posterior third of dorsum keels darker than background scale color; all dorsal scales without apical pits; vertebral scales slightly enlarged (1 medial row); outermost dorsal scale row not enlarged; ventrals VEN 185, with rounded outer margins, without lateral keels; anal plate entire, crescent in shape; subcaudals SC 76 (excluding terminal spine), all divided/paired; terminal caudal scale forming acuminated tail cap.

Coloration. Main background color of dorsal surfaces of head, body and tail ochre to yellowish-brown, graduating slightly lighter (light-ochre) on flanks; ventral surfaces of body and head yellowish-white to cream, chin off-white. Vertebral scales slightly brighter, light-bronze in color. Dorsals with minute dark brown dots, forming dusty pattern; dots scarce on flanks, much less dense on ventral scales. Main dorsal pattern consisting of 50 vertical, slightly billowing dark-brown bars (ca. 1–2 scales wide), in contact with vertebral scale row, extending to belly but normally not reaching ventrals ca. 1 scale. These bars continuing on tail (10), where they become incomplete and form irregular blotches gradually reducing posteriorly, continuing to interrupted lateral dark stripes (height ca. 1 scale) from second half of tail to tail tip. Ventrals with rare irregular dark-grey to dark-brown spots, being more densely scattered on lateral sides of ventrals forming interrupted lines. Head with minute dark dots, denser on dorsal and lateral surfaces, nearly absent on the underside. Numerous

brownish-black irregular spots and blotches (size < 0.8–1 mm) covering dorsal surfaces of head, most numerous at central and medial portions of parietals, frontal, medial parts of supraorbitals, posterior part of prefrontals (along frontal scale contact). Dorsal surface of head appear darker than flanks, with occasional black blotches located on internasals, nasals, suboculars, and chin shields. Two dark stripes on each side running from the upper portion of postorbital backwards to parietal, upper anterior and posterior temporal, continuing on dorsal scales of neck, joining with two shorter stripes lasting from posterior ends of parietals; the whole pattern of dark stripes on dorsal side of head basis resembling “W”-shape. Dark stripes continuing backwards and joining wide dark stripe ca. 8 scales posteriorly from edge of parietals; the latter joining the first pair of lateral vertical dark bars. Two dark stripes beginning at lower portion of postorbital, running ventrally and posteriorly towards lower temporals to supralabial VII. Two large elliptical dark blotches on ventro-lateral sides of neck on both sides, at mouth angles and ca. 4–6 scales posteriorly to mouth angles. Nasal pinkish, with two small dark spots above naris. Iris orange-yellow with light-brownish periphery.

In alcohol, body brownish-grey, vertebral region yellowish-beige; dorsal blotches and head markings dark brownish-grey; lateral speckling dark brown; throat, venter and tail underside off-white, dark spots on ventral scales grey.

Description and variation of the paratype series.

External morphology. The most important characters of the available specimens, comprising the type series and referred materials, appear in Table 1. All other morphological characters agree with those described for the holotype.

Dentition. Two studied specimens (NMNS 05594 and ZMMU R-14434) had well-developed palatine dentition; both have 6 functional teeth on the left and 6–7 teeth on the right maxilla, and 11–13 teeth on left and 20 teeth on right lower jaw; teeth get gradually smaller posteriorly (Supplementary Table S3).

Body scalation. All scales are rhomboid; first and second median dorsal scale rows slightly enlarged, the vertebral row slightly differ in size and shape from other medial dorsal rows. Vertebral scale row always keeled, slight keels also notable on 0–3 median scale rows in anterior part of body; keels present on 5–9 median scale rows at midbody and posterior part of body. DSR: 15-15-15. Ventrals: 174–188, plus 1 (in one case 2 and in one case 3) preventrals; SC: 71–77, all paired; anal plate entire.

Head scalation. Generally as for holotype; single loreal and preocular, single postocular not fused with subocular, supralabials not contacting eye; supralabials 7–8/7–8, infralabials 8–9/8–9 (in two specimens ZMMU R-14434 and NMNS 05595 asymmetric condition 8/9 is observed) with one exception (7/7). Significant variability observed in temporal scales, 2+3/2+3 being the most common condition (36% of available specimens), however small subrectangular scales often appear among posterior temporals on one or other side of head, resulting asymmetric conditions 2+3/2+4 or 2+4/2+3 being quite common (observed in 36% of samples). Two specimens (NMNS 05586 and ZMMU R-14436) show additional anterior temporals (conditions 3+3/2+3 and 2+3/3+4 respectively), whereas the other specimen (ZMMU R-14434) shows only two posterior temporals on each head side (condition 2+2/2+2). Finally, in one specimen on one side of the head only single anterior temporal is present (condition 1+3/2+4).

Coloration. Coloration in life largely corresponds to that of holotype (Fig. 4A–4C); background color may vary from yellowish-brown to darker bronze-orange; degree of development of dark blotches, bars and spots also may vary. Paratypes NMNS 05587, 05593, and ZMMU R-14435 are darker than holotype, dark lateral stripes run from temporal region posteriorly on ca. 1 head length joining two pairs of dark vertical bars on both sides of neck. Paratype ZMMU R-14436 has slightly darker overall coloration due to denser black speckling on dorsal scales and the head.

Hemipenis. (Description based on 2 paratype males: ZMMU R-14435 and ZMMU

R-14436). Hemipenis symmetrical, bilobed, forked, the surface from base to crotch nude, with numerous (8–12) shallow folds on the sulcal surface and 4–5 larger dermal ridges on the asulcal surface (Supplementary Fig. S5). Sulcus spermaticus deep, with fleshy swollen edges, bifurcate into two separate canals towards or on the apical lobes. Apical lobes with well-developed ornamentation, covered with large fleshy irregularly curved folds in 4–5 rows and fleshy protuberances, separated with deep slits and forming complex pattern resembling brain cortex.

Natural history notes.

Pareas atayal inhabits various types of forests at altitudes of ca. 100–2000 m above sea level. The new species feeds on a variety of land snails and slugs. In captivity, they were observed to prey on Bradybaenidae (several species of *Acusta* spp., *Bradybaena similaris*, and young *Nesiohelix swinhoei*), Camaenidae (*Satsuma mellea*, *S. nux*, and *S. viridibasis*), Philomycidae (*Meghimatium bilineatum* and *M. fruhstorferi*), and occasionally Ariophantidae (*Parmarion martensi*) (Jia-Wei Lin, personal communication on his master thesis, 2010). Strictly nocturnal, mostly active after twilight around 20:00, and is especially active after heavy rains when their prey is abundant. Usually recorded on branches of bushes and trees ca. 1–2 m above the ground. The active period lasts approximately from March to October, can also be found occasionally in winter. Excluding the northernmost tip of Taiwan, the species is widely found in sympatry with *P. formosensis*, and in Nantou County also in sympatry with *P. komaii*.

Distribution.

The new species is endemic to Taiwan. To date, *Pareas atayal* is confined to Taipei and New Taipei City, Yilan, Taoyuan, Hsinchu and Nantou counties of Taiwan. The discovery of new populations is also anticipated in Miaoli and Taichung counties. *Pareas atayal* inhabits

Datun and Xueshan Mountain Ridges, and the northwestern slopes of the Central Mountain Ridge. Although the southern boundary of its distribution is unclear, the new species was never recorded south of the Tropic of Cancer, as well as on eastern slopes of the Central Mountain Ridge.

Comparisons.

The new species *Pareas atayal* sp. nov. shares most morphological characters of scalation and coloration with closely related species of *Pareas* from East Asian islands (*P. formosensis, P. iwasakii, P. komaii*) and mainland Southeast Asia (*P. hamptoni*). The new species can be diagnosed from other congeners in the following way (Supplementary Table S4).

In having no contact between loreal and eye the new species can be differentiated from *P. boulengeri* (C and E China), *P. monticola* (NE India, Yunnan, N Vietnam) and *P. stanleyi* (C and E China) (loreal contacts eye in these taxa). In having prefrontal scale in contact with eye *Pareas atayal* sp. nov. is distinguished from *P. carinatus* (Indonesia, Malaysia, Indochina, Thailand, Myanmar, Yunnan; prefrontal not in contact with eye). The entire nasal distinguishes the new species from *P. nuchalis* (Borneo) and *P. stanleyi* (nasal divided in these species). In having separate subocular and single postorbital not fused *Pareas atayal* sp. nov. can be diagnosed from a number of species, including *P. boulengeri*, *P. margaritophorus* (Thailand, Myanmar, Indochina, S China), *P. nigriceps* (Yunnan) and *P. nuchalis* (subocular and postorbital fused in these taxa). It is noteworthy that the holotype of *P. hamptoni* from Mogok (Myanmar) according to the original description by Boulenger (1905) also shows fused subocular and postorbital scales, whereas the examined specimens of *P. hamptoni* from Indochina (sometimes referred as *P. h. tonkinenesis* - see Orlov et al., 2002, Nguyen et al., 2009) had separate subocular and single postorbital not fused. In having two anterior temporals the new species is further differentiated from the holotype of *P. hamptoni* from

Myanmar, *P. monticola* and *P. nigriceps* (all have single anterior temporal), as well as from *P. carinatus* and *P. nuchalis* (both have three anterior temporals).

From *P. formosensis* in Taiwan and *P. hamptoni* in Southeast Asian mainland, the new species can be diagnosed by the following combination of morphological attributes (Table 1): (1) in having 7 median dorsal scale rows with notable keels (vs. dorsals completely smooth in *P. formosensis*, dorsals smooth or with weak keel in 1 medial row in *P. hamptoni*); (2) in having yellowish coloration of iris (vs. iris bright orange to red in *P. formosensis* and *P. hamptoni*); (3) in having much longer head, HL/TL ratio 0.035 ± 0.003 in *P. atayal* (vs. HL/TL ratio 0.029 ± 0.002 in *P. formosensis*, also see supplementary Fig. S1); (4) in having comparatively much shorter rostral part of head: SnL/HL ratio 0.24 ± 0.02 in *P. atayal* (vs. SnL/HL ratio 0.29 ± 0.02 in *P. formosensis*); (5) in having higher numbers of infralabials (8.59 ± 0.59 vs. 6.65±0.59) and ventrals (180.77 ± 4.55 vs. 174.85 ± 3.08); (6) in having less intense dark mottling on dorsal surfaces of head: in *P. atayal* (Fig. 4A–4C) comparatively larger black spots covering mostly central parts of parietals and frontal scales (normally 8–14 spots in head cross-section), being much less abundant on lateral sides of parietals, suboculars and prefrontals (vs. numerous small dark dots cover dorsal surfaces of head almost uniformly (normally over 20-24 per head cross-section), continuing to lateral sides of the head, thus appearing darker in *P. formosensis* (Fig. 4G–4I) and *P. hamptoni*).

From the other yellow-eyed Taiwanese species, *P. komaii*, the new species can be distinguished by: (1) having less keeled dorsals: 5 to 9 middorsal scale rows at midbody and posterior part of body show keels in *P. atayal* (vs. from 7 to 13 scale rows at midbody and from 9 to 13 scale rows at posterior part of body bearing well-pronounced keels in *P. komaii*); (2) anterior part of body normally lacking keeled dorsals, from 0 to 3 scale rows with keels (mean KAD 0.47 ± 1.01) in the new species (vs. well-keeled dorsals at anterior part of body in *P. komaii*, mean KAD 4.82 ± 2.15); (3) having higher numbers of ventrals (180.77 ± 4.55 vs. 174.27 ± 4.67) and subcaudals (75.47 ± 2.23 vs. 69.56 ± 3.84); (4) *P. atayal* has lighter

background coloration with more pronounced dark transverse bands (Fig. 4A–4C), vs. normally darker background coloration with less distinct transverse dark bands in *P. komaii*, (Fig. 4D–4F).

Among all other *Pareas* the new species morphologically most closely resembles the Okinawan species *P. iwasakii* (Fig. 4J–4L). However, the new species can be diagnosed from *P. iwasakii* on the basis of the following morphological features: (1) a comparatively less elongated head in *P. atayal*, SnL/HL ratio 0.24 ± 0.02 (vs. SnL/HL ratio 0.20 ± 0.01 in *P. iwasakii*); (2) smaller number of ventrals, VEN 174–188 (180.77 ± 4.55) in *P. atayal* vs. VEN 188–199 (192.00 ± 1.41) in *P. iwasakii*, according to Ota *et al.* (1997b) and our original data; (3) larger number of enlarged vertebral scale rows: 3 middorsal scale rows enlarged in *P. atayal* (vs. 1 middorsal scale row enlarged in *P. iwasakii*); (4) usually smaller number of infralabials, 7–9 (8.59 ± 0.59) in *P. atayal* (vs. 9–11 (9.75 ± 0.87) in *P. iwasakii*); (5) normally smaller number of subcaudals, 71–79 (75.47 ± 2.23) in *P. atayal* (vs. 76–84 (79.00 ± 3.83) in *P. iwasakii*).

Supplementary Table S1 Sample ID, original and revised identification of species, sample locality, GenBank accession number, and source of specimens used in this study. Abbreviation of each sample locality (within the parentheses) corresponds to that in Fig. 1.

Species	ID	Sample locality	GenBank Accession No.		Source	Taxonomic revision
			Cytochrome *b*	C-mos		
P. formosensis	NMNS 05584*	(A) Yangmingshan, Taipei, TW	KJ642114	KJ642198	This study	*P. atayal* sp.nov.
yellow-eyed form,	NMNS 05585*	(A) Yangmingshan, Taipei, TW	KJ642115	KJ642198	This study	*P. atayal* sp.nov.
weekly keeled dorsals	NMNS 05586*	(A) Yangmingshan, Taipei, TW	KJ642116	KJ642198	This study	*P. atayal* sp.nov.
	HC 000711	(A) Yangmingshan, Taipei, TW	JF827688	JF827714	Guo *et al.*, 2011	*P. atayal* sp.nov.
	NMNS 05587*	(B) Shiding, Taipei, TW	N/A	N/A	This study	*P. atayal* sp.nov.
	NMNS 05588*	(B) Sanxia, Taipei, TW	KJ642117	KJ642198	This study	*P. atayal* sp.nov.
	NMNS 05589*	(B) Wulai, Taipei, TW	KJ642118	KJ642198	This study	*P. atayal* sp.nov.
	NMNS 05590	(B) Wulai, Taipei, TW	KJ642119	KJ642198	This study	*P. atayal* sp.nov.
	NMNS 05591*	(B) Wulai, Taipei, TW	N/A	N/A	This study	*P. atayal* sp.nov.
	NMNS 05592	(C) N. Cross-Is. Highway, TW	KJ642120	KJ642199	This study	*P. atayal* sp.nov.
	NMNS 05593*	(C) N. Cross-Is. Highway, TW	KJ642121	KJ642198	This study	*P. atayal* sp.nov.
	NMNS 05594**	(C) N. Cross-Is. Highway, TW	KJ642122	KJ642198	This study	*P. atayal* sp.nov.
	ZMMU R-14434*	(C) N. Cross-Is. Highway, TW	KJ642123	KJ642198	This study	*P. atayal* sp.nov.
	NMNS 05595*	(C) N. Cross-Is. Highway, TW	KJ642124	KJ642198	This study	*P. atayal* sp.nov.
	ZMMU R-14435*	(C) N. Cross-Is. Highway, TW	KJ642125	KJ642198	This study	*P. atayal* sp.nov.
	ZMMU R-14436*	(C) N. Cross-Is. Highway, TW	N/A	N/A	This study	*P. atayal* sp.nov.
	HC 000618	(C) N. Cross-Is. Highway, TW	JF827685	JF827711	Guo *et al.*, 2011	*P. atayal* sp.nov.
	HC 000628	(C) N. Cross-Is. Highway, TW	JF827686	JF827712	Guo *et al.*, 2011	*P. atayal* sp.nov.
	NMNS 05596*	(F) Xitou, Nantou, TW	KJ642126	KJ642198	This study	*P. atayal* sp.nov.
	NMNS 05597	(F) Xitou, Nantou, TW	KJ642127	KJ642198	This study	*P. atayal* sp.nov.
P. formosensis	NMNS 05600	(D) Daxueshan, Taichung, TW	KJ642161	KJ642210	This study	*P. komaii*
yellow-eyed form,	NMNS 05598	(D) Daxueshan, Taichung, TW	KJ642162	KJ642210	This study	*P. komaii*
strongly keeled dorsals	NMNS 05599	(D) Daxueshan, Taichung, TW	KJ642163	KJ642210	This study	*P. komaii*
	NTNU-LHX1	(E) Sun Moon Lake, Nantou, TW	KJ642164	KJ642210	This study	*P. komaii*
	NMNS 05601	(E) Sun Moon Lake, Nantou, TW	KJ642165	KJ642210	This study	*P. komaii*
	NMNS 05602	(E) Sun Moon Lake, Nantou, TW	KJ642166	KJ642210	This study	*P. komaii*
	NMNS 05603	(F) Xitou, Nantou, TW	KJ642167	KJ642210	This study	*P. komaii*
	NMNS 05604	(F) Xitou, Nantou, TW	KJ642168	KJ642210	This study	*P. komaii*
	NMNS 05605	(H) Mailing, Chiayi, TW	KJ642169	KJ642210	This study	*P. komaii*
	NMNS 05606	(I) Taiwu, Pingdong, TW	KJ642170	KJ642210	This study	*P. komaii*
	NMNS 05607	(I) Taiwu, Pingdong, TW	KJ642171	KJ642210	This study	*P. komaii*
	NMNS 05608	(I) Taiwu, Pingdong, TW	KJ642172	KJ642210	This study	*P. komaii*
	NMNS 05609	(I) Taiwu, Pingdong, TW	KJ642173	KJ642210	This study	*P. komaii*
	NMNS 05610	(I) Taiwu, Pingdong, TW	KJ642174	KJ642210	This study	*P. komaii*
	NMNS 05611	(J) Dahanshan, Pingdong, TW	KJ642175	KJ642210	This study	*P. komaii*
	NMNS 05612	(J) Dahanshan, Pingdong, TW	KJ642176	KJ642210	This study	*P. komaii*
	NMNS 05613	(J) Dahanshan, Pingdong, TW	KJ642177	KJ642210	This study	*P. komaii*
	NMNS 05614	(J) Dahanshan, Pingdong, TW	KJ642178	KJ642210	This study	*P. komaii*
	NMNS 05615	(J) Dahanshan, Pingdong, TW	KJ642179	KJ642210	This study	*P. komaii*
	NMNS 05616	(J) Dahanshan, Pingdong, TW	KJ642180	KJ642210	This study	*P. komaii*
	NMNS 05617	(K) Taimali, Taidong, TW	KJ642181	KJ642211	This study	*P. komaii*
	NMNS 05618	(L) Lijia, Taidong, TW	KJ642182	KJ642210	This study	*P. komaii*
	NMNS 05619	(L) Lijia, Taidong, TW	KJ642183	KJ642210	This study	*P. komaii*
	NMNS 05620	(L) Lijia, Taidong, TW	KJ642184	KJ642210	This study	*P. komaii*
	NMNS 05621	(L) Lijia, Taidong, TW	KJ642185	KJ642210	This study	*P. komaii*
	NMNS 05622	(L) Lijia, Taidong, TW	KJ642186	KJ642210	This study	*P. komaii*
	NMNS 05623	(L) Lijia, Taidong, TW	KJ642187	KJ642212	This study	*P. komaii*
	NMNS 05624	(L) Lijia, Taidong, TW	KJ642188	KJ642210	This study	*P. komaii*
	NMNS 05625	(M) Ruisui, Hualien, TW	KJ642189	KJ642210	This study	*P. komaii*
	NMNS 05626	(M) Ruisui, Hualien, TW	KJ642190	KJ642210	This study	*P. komaii*
	NMNS 05627	(M) Ruisui, Hualien, TW	KJ642191	KJ642213	This study	*P. komaii*
	NMNS 05628	(M) Ruisui, Hualien, TW	KJ642192	KJ642210	This study	*P. komaii*
	NMNS 05629	(N) Wanrong, Hualien, TW	KJ642193	KJ642210	This study	*P. komaii*
	NMNS 05630	(N) Wanrong, Hualien, TW	N/A	N/A	This study	*P. komaii*
	NMNS 05631	(O) Chungde, Hualien, TW	KJ642194	KJ642210	This study	*P. komaii*
	HC 000669	(L) Lijia, Taidong, TW	JF827687	JF827713	Guo *et al.*, 2011	*P. komaii*
P. formosensis	NMNS 05632	(C) N. Cross-Is. Highway, TW	KJ642130	KJ642201	This study	*P. formosensis*
red-eyed form,	NMNS 05633	(C) N. Cross-Is. Highway, TW	KJ642131	KJ642201	This study	*P. formosensis*
smooth dorsals	NMNS 05634	(C) N. Cross-Is. Highway, TW	KJ642132	KJ642201	This study	*P. formosensis*
	NMNS 05635	(D) Daxueshan, Taichung, TW	KJ642133	KJ642201	This study	*P. formosensis*
	NMNS 05636	(D) Daxueshan, Taichung, TW	KJ642134	KJ642201	This study	*P. formosensis*
	NTNU-LHR1	(E) Sun Moon Lake, Nantou, TW	KJ642135	KJ642201	This study	*P. formosensis*
	NMNS 05637	(F) Xitou, Nantou, TW	KJ642136	KJ642202	This study	*P. formosensis*
	NMNS 05638	(F) Xitou, Nantou, TW	KJ642137	KJ642201	This study	*P. formosensis*
	NMNS 05639	(F) Xitou, Nantou, TW	KJ642138	KJ642201/ KJ642203	This study	*P. formosensis*

	NMNS 05640	(F) Xitou, Nantou, TW	KJ642139	KJ642201/ KJ642203	This study	*P. formosensis*
	NMNS 05641	(F) Xitou, Nantou, TW	KJ642140	KJ642201	This study	*P. formosensis*
	NMNS 05642	(F) Xitou, Nantou, TW	KJ642141	KJ642201/ KJ642203	This study	*P. formosensis*
	NMNS 05643	(G) Alishan, Jiayi, TW	KJ642142	KJ642201	This study	*P. formosensis*
	NMNS 05644	(G) Alishan, Jiayi, TW	KJ642143	KJ642204	This study	*P. formosensis*
	NMNS 05645	(I) Taiwu, Pingdong, TW	KJ642144	KJ642203	This study	*P. formosensis*
	NMNS 05646	(I) Taiwu, Pingdong, TW	KJ642145	KJ642203	This study	*P. formosensis*
	NMNS 05647	(I) Taiwu, Pingdong, TW	KJ642146	KJ642201/ KJ642203	This study	*P. formosensis*
	NMNS 05648	(J) Dahanshan, Pingdong, TW	KJ642147	KJ642203	This study	*P. formosensis*
	NMNS 05649	(J) Dahanshan, Pingdong, TW	KJ642148	KJ642203	This study	*P. formosensis*
	NMNS 05650	(J) Dahanshan, Pingdong, TW	KJ642149	KJ642201/ KJ642203	This study	*P. formosensis*
	NMNS 05651	(J) Dahanshan, Pingdong, TW	KJ642150	KJ642201/ KJ642203	This study	*P. formosensis*
	NMNS 05652	(L) Lijia, Taidong, TW	KJ642151	KJ642201/ KJ642203	This study	*P. formosensis*
	NMNS 05653	(L) Lijia, Taidong, TW	KJ642152	KJ642203	This study	*P. formosensis*
P. formosensis	CIB 010140	Baoxing, Sichuan, China	JF827690	JF827716	Guo *et al.*, 2011	*P. chinensis*
Population in China	CIB 098269	Tianquan, Sichuan, China	JF827691	JF827717	Guo *et al.*, 2011	*P. chinensis*
	CIB 010141	Baoxing, Sichuan, China	JF827692	JF827718	Guo *et al.*, 2011	*P. chinensis*
	CIB 010144	Baoxing, Sichuan, China	JF827693	JF827719	Guo *et al.*, 2011	*P. chinensis*
	CIB 098272	Tianquan, Sichuan, China	JF827694	JF827720	Guo *et al.*, 2011	*P. chinensis*
	N/A	Xingou, Sichuan, China	HQ528535	N/A	Ding *et al.*, 2011	*P. chinensis*
P. hamptoni	NAP-01397	Bidoup Mt., Lam Dong, Vietnam	KJ642153	KJ642205	This study	*P. hamptoni*
	NAP-01714	Bidoup Mt., Lam Dong, Vietnam	KJ642154	KJ642205	This study	*P. hamptoni*
	H26-HAM01	Guangdong, China	KJ642155	KJ642201/ KJ642206	This study	*P. hamptoni*
	FMNH 258687	N/A	AY425809	N/A	Fernandesand Malhotra, unpublished	*P. hamptoni*
P. hamptoni tonkinensis	FMNH 255567	N/A	AY425806	N/A	Fernandesand Malhotra, unpublished	*P. hamptoni*
P.iwasakii	NMNS 05654	(P) Iriomote Is., S. Ryukyu, Japan	KJ642156	KJ642207	This study	*P. iwasakii*
	I02-IRI2	(P) Iriomote Is., S. Ryukyu, Japan	KJ642157	KJ642208/ KJ642209	This study	*P. iwasakii*
	I03-ISG1	(Q) Ishigaki Is., S. Ryukyu, Japan	KJ642158	KJ642207	This study	*P. iwasakii*
	I04-ISG2	(Q) Ishigaki Is., S. Ryukyu, Japan	KJ642159	KJ642207	This study	*P. iwasakii*
	I05-ISG3	(Q) Ishigaki Is., S. Ryukyu, Japan	KJ642160	KJ642198/ KJ642207	This study	*P. iwasakii*
	NMNS 05655	(Q) Ishigaki Is., S. Ryukyu, Japan	N/A	N/A	This study	*P. iwasakii*
P. boulengeri	KIZ 09965	Enshi, Hubei, China	JF827678	JF827704	Guo *et al.*, 2011	
	KIZ 09966	Jiannan, Hubei, China	JF827679	JF827705	Guo *et al.*, 2011	
	KIZ 09967	Jianzhuxi, Hubei, China	JF827680	JF827706	Guo *et al.*, 2011	
	KIZ 09968	Luxi, Hunan, China	JF827681	JF827707	Guo *et al.*, 2011	
	KIZ 09969	Shennongjia, Hubei, China	JF827682	JF827708	Guo *et al.*, 2011	
	KIZ 09970	Luxi, Hunan, China	JF827683	JF827709	Guo *et al.*, 2011	
	KIZ 09971	Shennongjia, Hubei, China	JF827684	JF827710	Guo *et al.*, 2011	
P. stanleyi	HM 2007-S001	Guilin, Guangxi, China	JN230704	JN230703	Guo *et al.*, 2011	
P. margaritophorus	NAP-00303	Bu Gia Map, Binh Phuok, Vietnam	KJ642195	KJ642214/ KJ642215	This study	
	NAP-00769	Bu Gia Map, Binh Phuok, Vietnam	KJ642196	KJ642215/ KJ642216	This study	
	N/A	Hongkong, China	KJ642197	KJ642217	This study	
	CIB 098267	Hainan, China	JF827675	JF827700	Guo *et al.*, 2011	
P. macularius	CAS 206620	Bago Division, Myanmar	AF471082	AY471150	Guo *et al.*, 2011	
P. monticola	SYN U04(II)149	Motuo, Xizang, China	JF827689	JF827715	Guo *et al.*, 2011	
P. carinatus	NAP-00065	Cat Tien, Dong Nai, Vietnam	KJ642128	KJ642200	This study	
	NAP-00066	Cat Tien, Dong Nai, Vietnam	KJ642129	KJ642200	This study	
	CIB 098270	Menla, Yunnan, China	JF827676	JF827701	Guo *et al.*, 2011	
	DL 2008-S039	Malaysia	JF827677	JF827702	Guo *et al.*, 2011	
Asthenodipsas vertebralis	N/A	Malaysia	AY425807	N/A	Fernandesand Malhotra, unpublished	
Asthenodipsas tropidonotus	N/A	Indonesia	AY425808	N/A	Fernandesand Malhotra, unpublished	
Aplopeltura boa	KIZ 011963	Malaysia	JF827673	JF827696	Guo *et al.*, 2011	

**: Holotype of *P. atayal* sp. nov.

*: Paratypes of *P. atayal* sp. nov.

Supplementary Table S2 Between-species divergence (upper-right) and within-species polymorphism (diagonal) among Taiwanese *Pareas* and their sister clade from mitochondrial cytochrome *b* sequences (in p-distance).

	P. atayal	*P. iwasakii*	*P. komaii*	*P. formosensis*	*P. hamptoni*	*P. boulengeri*	*P. chinensis*	*P. stanleyi*
P. atayal	0.0024	0.0823	0.1085	0.1810	0.1885	0.2105	0.2112	0.2230
P. iwasakii		0.0093	0.0994	0.1682	0.1809	0.2040	0.2086	0.2180
P. komaii			0.0313	0.1759	0.1897	0.2173	0.2090	0.2022
P. formosensis				0.0091	0.0571	0.1820	0.1905	0.2227
P. hamptoni					0.0513	0.1960	0.2108	0.2336
P. boulengeri						0.0014	0.1013	0.1702
P. chinensis							0.0000	0.1674
P. stanleyi								0.0000

Supplementary Table S3 Mandibular teeth count and asymmetry index for *Pareas atayal* sp. nov., *P. formosensis* and *P. komaii*. Calculation of asymmetry index follows Hoso *et al.* 2007.

Species	Sample locality	Right	Left	Index
P. atayal sp. nov.	Taoyuan (holotype)	20	11	29.03
P. atayal sp. nov.	Taoyuan (paratype)	20	13	21.21
P. formosensis	Pingdong	18	13	16.13
P. komaii	Hualien	21	16	13.51
P. komaii	Taidong	21	18	7.69

Supplementary Table S4 Diagnostic features of scalation and color pattern of currently recognised species of *Pareas* (based on Guo & Deng (2009), expanded and corrected). Exceptional values are shown in parentheses. Includes data from Pope (1935), Smith (1943), Nakamura & Uéno (1963), Taylor (1963), Rao & Yang (1992), Manthey & Grossmann (1997), Ota *et al.* (1997a), Ota *et al.* (1997b), Cox *et al.* (1998), Stuebing & Inger (1999), Zhao *et al.* (1998), Huang (2004), Jiang (2004), and Guo & Deng (2009). Abbreviations: N: nasal; LoEC: loreal-eye contact; PrFEC: prefrontal-eye contact; SbO: suboculars; PoO: postoculars; IL: infralabials; Tmp: temporals; KMD: number of keeled dorsal scale rows at midbody; V: vertebral scales; VEN: ventrals; SC: subcaudals.

Species	N	LoEC	PrFEC	SbO	PoO	IL	Tmp	KMD	V	VEN	SC	Head and neck pattern	Distribution
P. atayal sp. nov.	1	-	+	1	1	7–9	2+4	5–9	3	174–188	71–77	2 black lines from postorbital, lower reaching mouth angle, upper going behind head basis and contacting with short black line on neck	N Taiwan
P. boulengeri	1	+	+	Fused	Fused	8 (7,9)	2+3 (1+2)	0	0	176–187	62–77	A black line from behind eye to angle of mouth	C and E China
P. carinatus	1	-	-	1 or 2	2 or 1	7	3+4 or 3+3	9–13	3	158–206	53–99	A black line from eye to nape, and another from behind eye to angle of mouth	Indonesia, Malaysia, Indochina, Thailand, Myanmar, Yunnan
P. formosensis	1	-	+	1	1	7–9	2+3	0	1–3	163–185	70–80	A black line from rear of the supraocular to neck, and another from lower anterior-temporal to angle of mouth	Taiwan
*P. h. hamptoni**	1	-	+	Fused	Fused	7–8	1+2	feebly keeled	1	197–202	96	Two black longitudinal streaks on the back of the head and nape	N Myanmar
*P. h. tonkinensis***	1	-	+	1	1	7	2+2 or 2+3	0–1	1–3	180–196	73–98	A black line from eye to nape, and another from behind eye to angle of the mouth	Indochina, S China

P. iwasakii	1	-	+	1	1	9–11	3+4 or 2+3	5–7	1	189–194	76–84	A vertical black line from behind eye to neck, another line from behind eye to angle of mouth and to chin	Yaeyama islands, Okinawa
P. komaii	1	-	+	1	1	6–9	3+4 or 2+3	9–13	3	162–182	60–76	2 black lines from postorbital, lower reaching mouth angle, upper going behind head basis and contacting with short black line on neck	S and E Taiwan
P. margaritophorus	1	-	+	Fused	Fused	7	2+2 or 3+3	0	0	136–160	32–58	A white or yellow collar present or absent	Thailand, Myanmar, Indochina, S China
P. monticola	1	+	+	1	1 or 2	8	1+2 or 2+3	0	1	190–196	86–72	A black line from eye to nape, and another from behind eye to angle of mouth	NE India, Yunnan, N Vietnam
P. nigriceps	1	-	+ or -	Fused	Fused	7	1+2 or 1+3	9	1	175	77	A big black oval patch on back of head, two round black spots on each side of head, a black nuchal band	Yunnan
P. nuchalis	2	-	+	Fused	Fused	8–9	3+3 or 3+4	9–13	1	195–213	105–113	Oblique black line from lower corner of eye to front edge of last upper labial, and usually a thin, vertical black line at rear of head	Borneo (Indonesia, Malaysia)
P. stanleyi	2	+	+	1	1	7 (8)	2+2 or 2+3	13	0	151–160	48–60	A big black spot on the back of the head which separates into two vertical black lines behind the neck; a black line from behind the eye	C and E China

* based on original description of the holotype by Boulenger (1905) and description by Ota *et al.* (1997).

** based on specimens from Southern China and Vietnem.

Supplementary Figure S1 Lateral (A and B) and dorsal (C) views of a *Pareas atayal* sp. nov. (up) and *P. formosensis* (down) with identical body length showed the difference in head length (jaw length) and head shape. Photographed by Chung-Wei You.

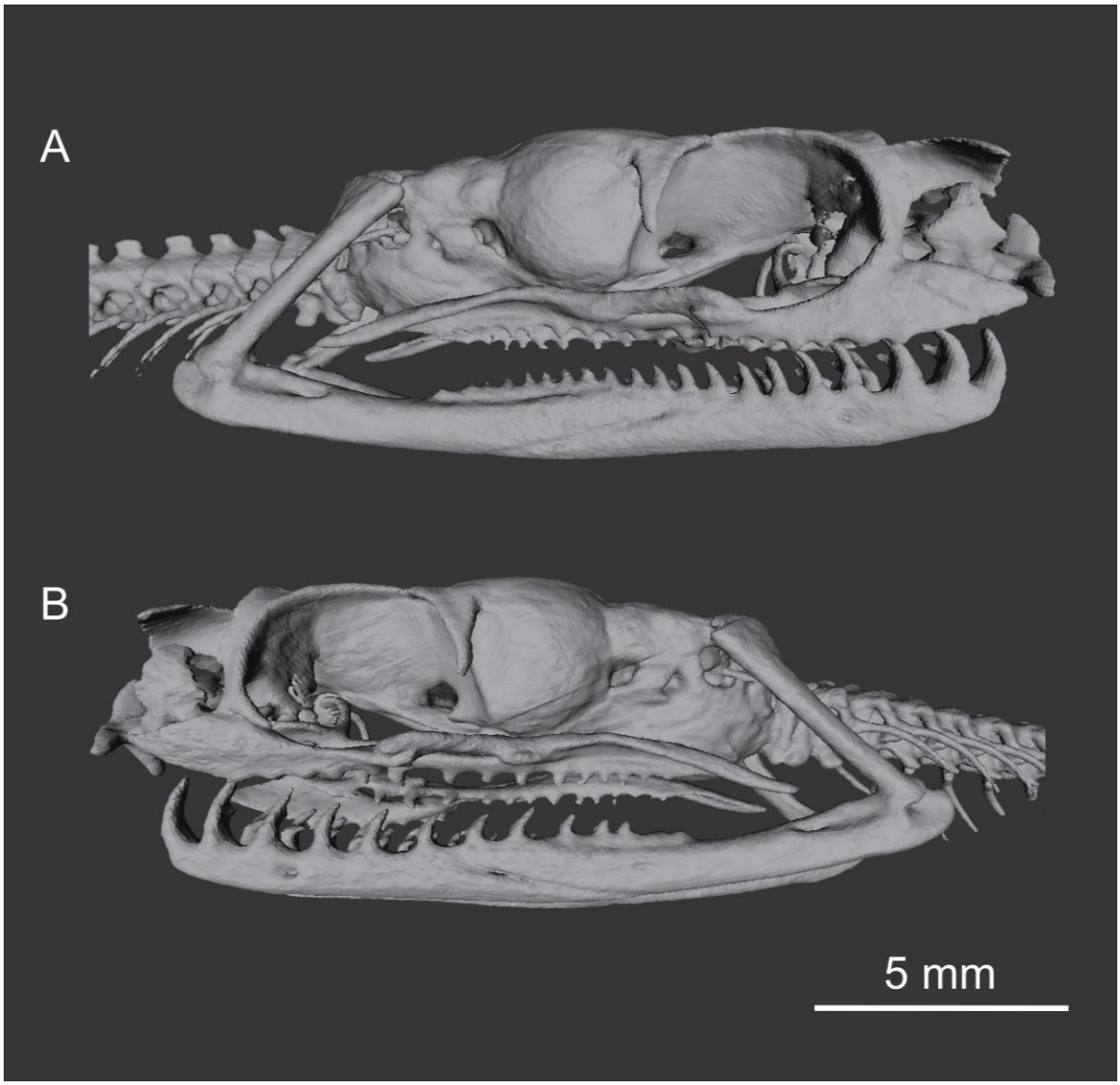

Supplementary Figure S2 Volume reconstruction of high-resolution X-ray computed tomography data showing cranium and mandibles of the holotype of *Pareas atayal* sp. nov., NMNS 05594. This figure was photographed and produced by Prof. Masaki Hoso, Kyoto University.

Supplementary Figure S3 Dorsal (A) and ventral (B) view of the holotype of *Pareas atayal* sp. nov., NMNS 05594. Photographed by Chung-Wei You.

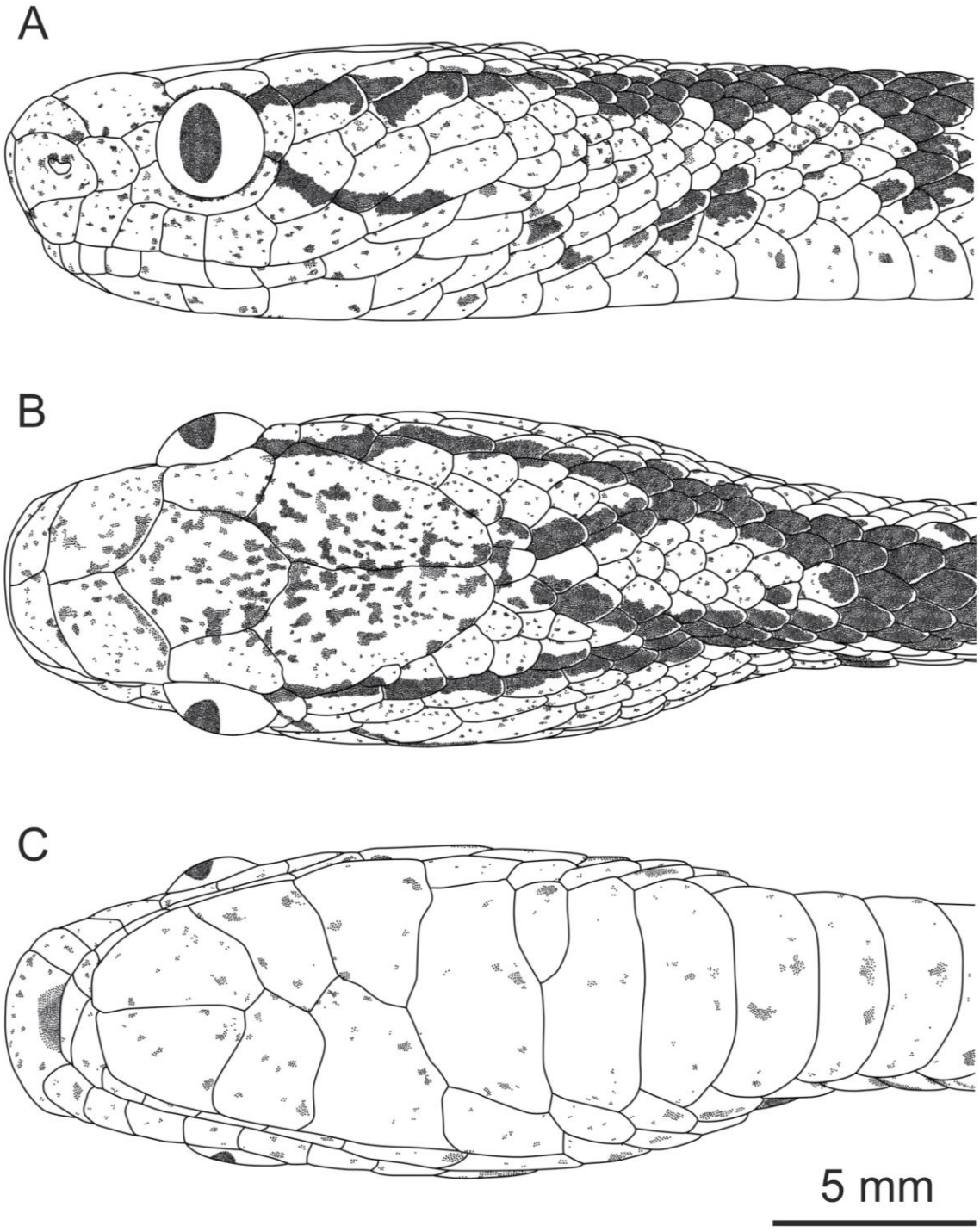

Supplementary Figure S4 Head scalation of the holotype of *Pareas atayal* sp. nov., NMNS 05594. (A) lateral, (B) dorsal, and (C) ventral views. Drew by Jia-Wei Lin.

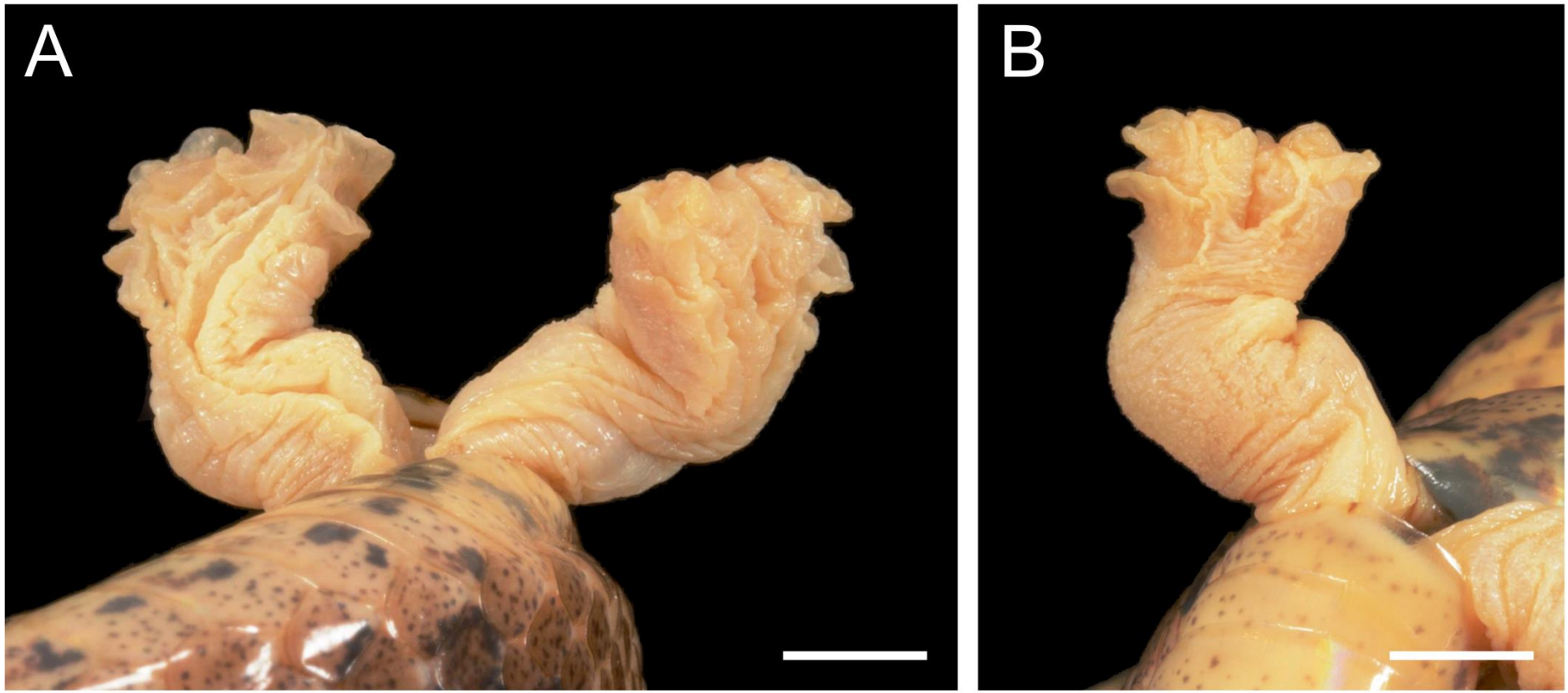

Supplementary Figure S5 Hemipenial sructures of *Pareas atayal* sp. nov. paratype ZMMU R-14435 from sulcal (A, left hemipenis), lateral (A, right hemipenis) and asulcal (B) sides. Scale bar equals to 5 mm. Photographed by Chung-Wei You.